

POLITECNICO DI TORINO

**Master's Degree in Communications and Computers
Networks Engineering**



Master's Degree Thesis

**Advanced 5G New Radio OFDM
Receivers for Single Frequency
Broadcast Networks**

Supervisors

Guido MONTORSI

Candidate

Mohsen EBNEALI

October 2021

Summary

In this thesis, delivering TV services to user devices is considered by investigating the possibility of using 5G New Radio (5G NR) OFDM numerology in the deployment of efficient Single Frequency Networks (SFNs).

SFNs are modeled with an equivalent channel characterized by a very large delay spread due to the typical inter-site distance (ISD) of the network. The straightforward approach in the design of the physical layer for the broadcasting application is based on the adoption of OFDM signaling with a very long OFDM symbol and very low sub-carrier spacing (SCS). This design choice allows to dimension the cyclic prefix length to eliminate ISI and ICI induced by the large delay spread with a consequent overhead reduction.

The 5G NR numerology, with a minimal SCS of 15 kHz and a maximum CP length of $4.7\mu\text{s}$, is designed for unicast transmission and Cyclic Prefix lengths are not compatible with those required for large SFN networks. As a consequence classical OFDM receiver based on single-tap equalizer provides unsatisfactory performance. First, we consider a general receiver based on the channel shortening principle, but in the frequency domain. The receiver consists of a bank of per tone time/frequency 2D filters, possibly followed by Maximum-Likelihood (ML) trellis processing on the shortened channel. We provide promising information-theoretic bound showing that the extension of 5G NR numerology to SFN is possible with very small performance loss. Even the simplest detector architecture that does not employ trellis processing provides throughput competitive with those that can be obtained with smaller SCS.

The results are based on the very strong assumption of perfect channel knowledge at the receiver and since the channel estimation in a mobile environment is a very critical function to the receiver performance, as the next step, we have considered designing a low complexity and adaptive 2-D channel MMSE equalizer which can acquire and track the ISI/ICI channel. The crucial parameter for complexity will be the number and positions of the required active taps in both dimensions and their trade-off with performance. The results showed the performance of the equalizer based on MSE criteria and also compared the performance by changing different parameters.

Acknowledgements

To my advisor, Professor Guido Montorsi, I would like to express my gratitude that he offered me the challenge to do my master thesis in wireless communications and mobile broadband networks and for his scientific guidance and strong support throughout this period. I wish to thank Dr. Majid Mosavat for his comments and suggestions regarding the optimization techniques that contributed to Chapter 3 of the thesis.

The support for this work was provided by the RAI-Radiotelevisione Italiana research center, which is hereby gratefully acknowledged. to all my professors at the Department of Electronic and Telecommunication for the scientific support and all my colleagues at CCNE group for the friendly atmosphere.

I would like to thank to my parents and my sister for their inexhaustible love and encouragement which was always available in the hard moments, despite the geographical distance between us. Finally, I would like to express my love to my fiancée, Naimeh, for the continuous support in the best and worst periods of the last years.

Table of Contents

List of Tables	VIII
List of Figures	IX
Acronyms	XII
1 Introduction	1
1.1 Introduction	1
1.2 5G Development Status	2
1.3 The Principle of Single Frequency Network	2
1.4 OFDM principles	3
1.4.1 The single-carrier modulation systems	4
1.4.2 Frequency division multiplexing modulation system	4
1.4.3 Orthogonality and FDM concept	4
1.4.4 A Simple Case of OFDM	5
1.4.5 Implementation of an OFDM system	5
1.4.6 Multipath channel distortion	7
1.4.7 Intersymbol Interference	7
1.4.8 Intercarrier Interference	8
2 Channel Equalization	10
2.1 introduction	10
2.1.1 Sequence Estimated-base Equalization Method	11
2.1.2 Filter-base Equalization Method	12
2.1.3 Linear equalization	13
2.1.4 Adaptive Algorithms	15
2.2 Channel Shortening	18
2.2.1 Optimal channel shortening	19
2.3 Implementation of 2-D Adaptive MMSE Equalizer for OFDM Systems With Insufficient Cyclic Prefix	20

3	Single Frequency Network Broadcasting with 5G NR Numerology	25
3.1	Introduction	25
3.2	SFN Network System for Broadcasting Transmission	26
3.3	optimal channel shortening performance	29
3.3.1	Simulation and result	29
3.3.2	Theoretical and Pragmatic achievable rate by $\tilde{\mathbf{H}}^r$ channel equalizer	30
3.3.3	Performances of realistic system	33
3.4	Performance of the 2-D Adaptive MMSE Equalizer	37
3.5	Conclusion and Future Work	43
	Bibliography	46

List of Tables

3.1	Different SFN networks and correspondent Delay Spread (DS) in LOS (TDL-E) and NLOS (TDL-A) channel models.	27
-----	---	----

List of Figures

1.1	Single Frequency Network. The whole transmitters operate at the same time and frequency. The nearest transmitters have more useful signals compared to the transmitters far from the receiver [2]. . . .	2
1.2	The spectrum of Single Carrier Spectrum Vs. MultiCarrier spectrum and OFDM. By OFDM and the Orthogonality property, it is possible to have more subcarriers in the same band compared to the multicarrier systems.	5
1.3	Overall spectrum of the OFDM signal with subcarriers within. The zero crossing all correspond to peaks of adjacent subcarriers. . . .	6
1.4	A block diagram of the OFDM system in transmitter and receiver.	6
1.5	Intersymbol Interference (ISI). a) OFDM symbol frame structure at transmitter side. b) OFDM symbol frame structure at the receiver side.	8
2.1	Transmitter and receiver and the equalization block	10
2.2	trellis diagram using in MLSE equalization	12
2.3	Block diagram of a linear equalizer made by the transversal FIR filter [4].	13
2.4	Block diagram of equalizer considering adaptive algorithm block [8].	15
2.5	Adaptive filter	16
2.6	Block diagram of an adaptive transversal filter with LMS algorithm.	17
2.7	From of the input of the 2-D equalizer	21
2.8	block diagram of a 2-D equalizer	22
2.9	p-norms of the unit vector[15].	23
2.10	Different shapes for active taps	23
3.1	System Model	27
3.2	Throughput efficiency versus ν for 5G NR numerologies with fixed SNR=5dB and $SCS = 2^\mu \times 15\text{kHz}$	30
3.3	Throughput efficiency T_E versus receiver complexity (ν) for 5G NR numerologies: TDL-A DS=50 μs (HPHT1, NLOS, 125km ISD) . . .	31

3.4	Throughput efficiency versus the sub-carrier spacing for 5G broadcasting, 5GNR numerologies and single carrier spacing with SNR=5dB; TDL-A DS=50 μ s (HPHT1, NLOS, 125km ISD)	33
3.5	Pragmatic capacity of QPSK, 16QAM and 64QAM inputs for single tap and 2D-MMSE equalizer	34
3.6	Simulated BER of the three considered realistic systems over TDL-A DS=50 μ s (HPHT1, NLOS, 125km ISD)	35
3.7	SNR thresholds (dB) at 1% BLER versus Delay spread of TDL-A channel model. Single Tap EQ. vs 2D-MMSE EQ. Code rate 0.53.	36
3.8	Mean Square Error versus the number of Iteration with same complexity for different shapes and different size of the window for OFDM system with "TDL-A channel model.	38
3.9	Mean Square Error versus the number of Iteration with the same size of window (8 \times 4) and different shape for OFDM system with "TDL-A" channel model with SNR=10dB; DS = 10e-6.	39
3.10	Mean Square Error versus the number of Iteration with different window size for Cross and Rectangular shape with OFDM system with "TDL-A" channel model with SNR=10dB; DS = 10e-6; step size = 0.01.	40
3.11	Mean Square error convergence for different learning rate.	41
3.12	Speed of convergence versus increasing the learning rate of equalizer (blue curve) and Residual MSE versus increasing the learning rate of equalizer (red curve) with SNR = 7dB and DS =10 μ s.	42
3.13	Comparison the Mean Square Error of the optimal EQ. vesus Adaptive 2-D MMSE EQ. for SNR = 7dB and DS =10 μ s.	43

Acronyms

5G NR

fifth Generation New Radio

OFDM

Orthogonal Frequency Division Multiplexing

SFN

Single Frequency Network

ISD

Inter-site Distance

SCS

Sub-carrier Spacing

ISI

Inter-symbol Interference

CP

Cyclic Prefix

MMSE

Minimum Mean Squared Error

CIR

Channel Impulse Response

LOS

Line of Sight

NLOS

Non Line of Sight

DS

Delay Spread

HPHT

High Power High Tower

MPMT

Medium Power Medium Tower

LPLT

Low Power Low Tower

MBS

Multimedia Broadcast Service

DVB-T2

second Generation Digital Video Broadcasting Terrestrial

ATSC

Advanced Television Systems Committee

3GPP

Third Generation Partnership Project

LTE

Long-Term Evolution

BER

Bit Error Rate

ZF

Zero-Forcing

MLSE

Maximum Likelihood Sequence Estimation

Chapter 1

Introduction

1.1 Introduction

Fourth-generation Long-Term Evolution (4G-LTE) and Fifth-generation (5G) cellular networks have expanded in different areas such as ultra-reliable low-latency communication (UR-LLC), massive machine-type communication (mMTC), Internet-of-Things (IOT), and many others in order to support new verticals besides mobile broadbands. Adaptation to different cases and requirements is possible thanks to using the flexible Orthogonal Frequency Division Multiplexing (OFDM)-based physical layer architecture of cellular networks.

Multimedia Broadcast Multicast Service (MBMS) is one of the expansions that shows the evolution of cellular networks in the realm of cellular broadcasting. MBMS has been part of the Third Generation Partnership Project (3GPP) specification since Release 6 in 2005 based on UTRAN. Then, the evolved version of MBMS has been introduced since Release 9 based on LTE which is referred to as "eMBMS". Based on dedicated requirements of broadcast services, 3GPP specifications have gradually evolved to support different broadcast services. Therefore, Release 14 was developed to enhance the service support and address the issues relevant to MBMS.

The scenarios for eMBMS services in 3GPP Release 14, based on LTE were expanded to include terrestrial broadcasting which is included new requirements such as Network dedicated to TV broadcast, Single Frequency Network (SFN) deployments with Inter-Site Distance (ISD) significantly larger than a typical ISD associated with typical cellular deployments and support for Receive-Only Mode (ROM) devices.

Despite the evolution in LTE eMBMS, there is some potential limitation in this type of network deployment. Supporting the requirements of different network deployments such as high mobility and high coverage in a large area is the issue

which both MBSFN and SC-PTM solutions in LTE eMBMS suffer these limitations.

1.2 5G Development Status

Release 15, which is the first 3GPP Release of 5G, has been proposed a flexible broadcast and multicast service as a feature that we can use in 5G deployments and requirements in 3GPP for next-generation access technologies. The evolution that took place in order to satisfy all the requirements of 5G cellular broadcast is referred to *LTE-based 5G Terrestrial Broadcast* in 3GPP Release 16 [1].

While in the initial release of LTE the MBSFN framework was supported which made the possibility of transmission of MBMS services over a large amount of geographical area, some Key ingredients were still required to support use cases as the competing broadcasting standards such as DVB-T2 and ATSC.

1.3 The Principle of Single Frequency Network

The possibility to overcome multi-path interference by using the OFDM concept allows distributing a program over all transmitters in a radio network using the same frequency. In SFN, the useful signal at the receiver is made by the superposition of all signals coming from those transmitters which is sent the signals synchronously.

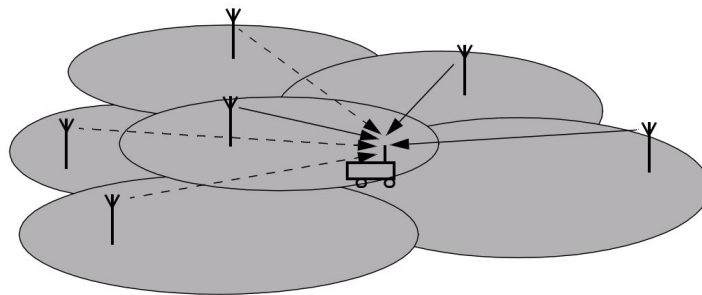


Figure 1.1: Single Frequency Network. The whole transmitters operate at the same time and frequency. The nearest transmitters have more useful signals compared to the transmitters far from the receiver [2].

The main advantages of SFN concept compared to the conventional multi-frequency networks are as follow:

- The most important advantage of the System using the SFN concept is high spectrum efficiency compared to the MFN approach. In a scarce spectrum environment, when the spectrum is occupied by analog services or when the

broadcasting services are getting more attractive for customers, spectrum efficiency is a major criterion that should be considered.

- As it is mentioned before, the received signal is the superposition of the signals coming from several transmitters which are sent the signals at the same time and frequency. Therefore, in the SFN system, the variation of the total field strength is lower and the location probability is higher than the single transmitter case. Consequently, Using the SFN concept prepared better network gain (or diversity gain).
- Due to the better network gain, the field strength distribution over the total service area is more homogeneous compared to MFN systems.
- Using dense SFN can guarantee the robustness of the system in which the failure of a single transmitter does not result in coverage outage for the whole network.

Besides the advantages, there are some disadvantages [2]:

- There is no possibility to do network splitting.
- It is necessary to have the time synchronization among transmitters
- The frequency synchronization is necessary in both transmitter and receiver sides. Otherwise we might lose orthogonality.

In the SFN concept, the received signal is the multiple copies of the transmitted signal with different delays. There are two types of dispersion. the first type occurs by the obstacles in the environment near to receiver which is "natural dispersion" and the second type drives from a difference in distance between transmitter antennas which is named "artificial dispersion". These delays should be considered in OFDM design in order to avoid inter-symbol interference.

In OFDM, the ISI is controlled by using a longer transmitted symbol than the actual interval observed by the receiver. Therefore, for avoiding inter-symbol interference, the guard interval should be larger than the delay spread. In this case, the delay of far transmitters should be considered because they can cause inter-symbol interference due to excessive delay.

1.4 OFDM principles

Although, for several decades, the Orthogonal Frequency Division Multiplexing (OFDM) modulation concept has existed, recently, the implementation of this concept for practical application is considering [3].

1.4.1 The single-carrier modulation systems

In single-carrier system, information is modulated by one carrier using frequency phase, or amplitude adjustment of the carrier. In digital systems, the information is in the form of bits. At higher bandwidth, the duration of one bit (or symbol) of information becomes smaller. Therefore, different types of impairments such as impulse noise or signal reflection can cause a significant loss of information.

1.4.2 Frequency division multiplexing modulation system

FDM is an extension which is using multiple subcarriers within the same bandwidth as the single carrier system. The total data rate is divided among the subcarriers.

There are some advantages compared to a single carrier system. It can be possible to use separate modulation and demodulation customized to a particular type of data. Moreover, sending out multiple dissimilar data is possible by multiple and different modulation schemes. FDM also offers another advantage in terms of narrowband frequency interference in which one of the frequency subbands will be affected by interference and the other subbands will be survived. Additionally, there is specific immunity to impairments due to a lower information rate and a longer data symbol period. The price of these advantages is losing effectiveness on information rate because of using the guard band in order to avoid interfering among the modulated subcarriers.

1.4.3 Orthogonality and FDM concept

Since, orthogonality among subcarriers result in eliminate the need of having guardbands, Adding this property to FDM systems makes a spectral efficiency with higher level. By orthogonality, the overlap of the subcarriers'spectra will be allowed and in spite of the overlapping, it is still attainable to retrieve the individual subcarriers' signals.

In order to make an orthogonal signal, It is necessary for the signals to have the inner product equal to zero. By referring to stochastic process, two random processes are orthogonal if they are uncorrelated [3]. In OFDM systems, the DFT transform is used to map the input signal onto a set of orthogonal basis functions of the DFT in transmitter and receiver. Since the basic functions of the DFT are uncorrelated, The correlation performed in the DFT for a given subcarrier only considers the energy for that corresponding subcarrier. Consequently, this separation of signal energy makes possibility of having the overlap among the OFDM subcarriers' spectrums without leading to make interference.

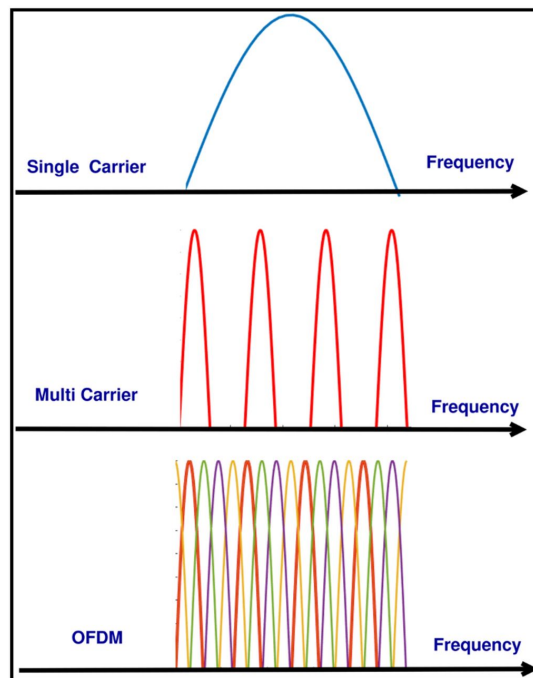


Figure 1.2: The spectrum of Single Carrier Spectrum Vs. MultiCarrier spectrum and OFDM. By OFDM and the Orthogonality property, it is possible to have more subcarriers in the same band compared to the multicarrier systems.

1.4.4 A Simple Case of OFDM

A simple representation of an OFDM frequency spectrum is depicted in Figure 1.3. The frequency of each subcarrier is selected in order to form an orthogonal signal set. These frequencies are known on the receiver side. In the frequency domain, the sin function side lobes produce overlapping spectra. It is necessary to mention that the individual peaks of subbands all line up with the zero crossings of other subbands. Therefore, there is no interference with the system during recovering the original signal. The receiver correlates the incoming signal by the known set of sinusoids to produce the original set of the data. This principle could be enhanced by using more complex modulation in the digital implementation of an OFDM system.

1.4.5 Implementation of an OFDM system

Representation of the OFDM system in digital domain which is an extension of the analog OFDM system is done by using the discrete Fourier transform (DFT) and its counterpart the inverse discrete Fourier transform (IDFT). In the OFDM system,

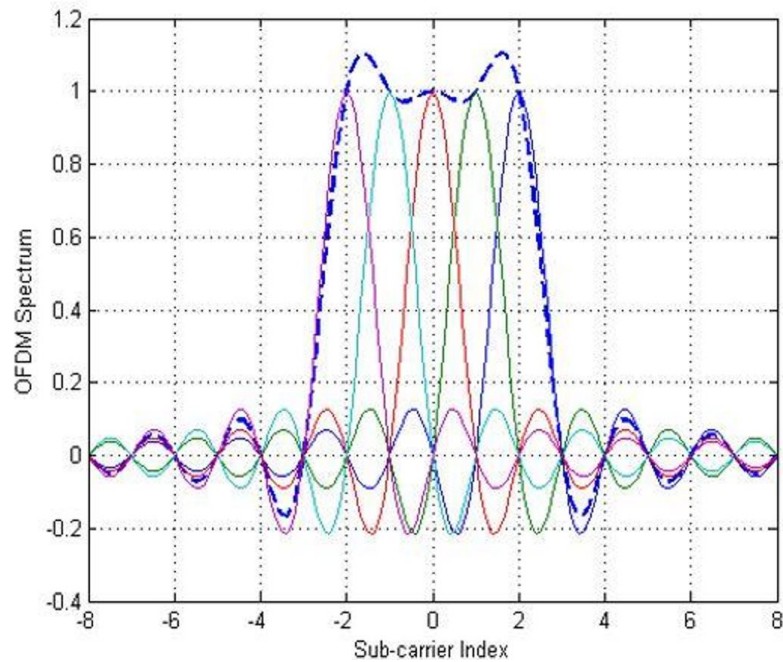


Figure 1.3: Overall spectrum of the OFDM signal with subcarriers within. The zero crossing all correspond to peaks of adjacent subcarriers.

These transforms are used in order to mapping data onto orthogonal subcarriers. These transforms are used for transforming data between the time-domain and frequency-domain. In order to implement the practical OFDM system, instead of DFT and IDFT, a combination of fast Fourier transform (FFT) and inverse fast Fourier transform (IFFT) is used which are mathematically equivalent versions of the DFT and IDFT, but more efficient to implement.

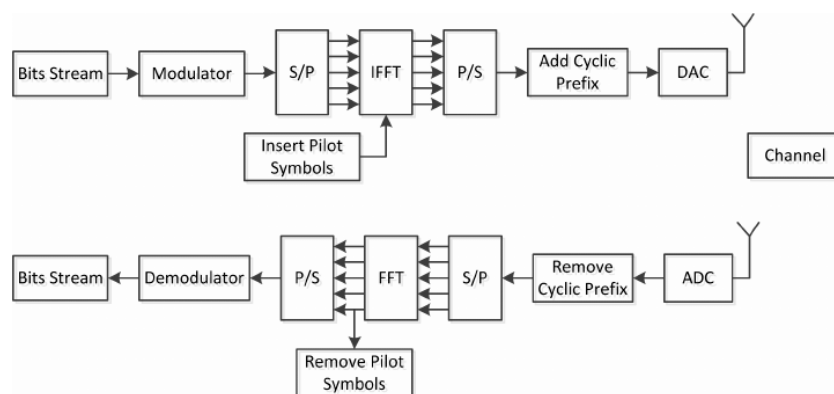


Figure 1.4: A block diagram of the OFDM system in transmitter and receiver.

Figure 1.4 shows a block diagram of a transmitter and receiver of an OFDM system. The system considers the source of the symbols which are the QPSK or QAM symbols as though they are in the frequency domain at the transmitter. The IFFT block takes these symbols as the input and brings the signal into the time domain. The IFFT takes the N symbols at a time where N is the number of the subcarriers in the system and these N symbols have a symbol period of T seconds. Each input symbol considers as a complex weight for the corresponding sinusoidal basis function. For an IFFT, the basis functions are N orthogonal sinusoids that have different frequencies. Since the input symbol is formed by a complex number, it is possible to determine both the amplitude and phase of the sinusoid for each subcarrier. The output of IFFT is the summation of all N subcarriers' sinusoidal signals which makes up a single OFDM symbol. The length of the OFDM symbol is NT where T is the IFFT input symbol period.

The output of the IFFT represents the time domain signal. After some additional processing, the signal is transmitted across the channel. At the receiver side, an FFT block is used in order to process the received signal. The output of TTF is the signal in the frequency domain and Ideally, it should be the original symbol that was sent to IFFT at the transmitter.

1.4.6 Multipath channel distortion

The presence of a multipath channel is a major problem in wireless communication systems. The reflection of the signal from different obstacles could make multipath delayed versions of the transmitted signal which leads to having a distorted signal at the receiver.

In OFDM systems, there are two kinds of problems due to the multipath channel. The first problem is InterSymbol Interference in which the OFDM received symbol will be distorted by the previously transmitted symbol. In typical OFDM systems, where the OFDM symbol period is much longer than the time span of the channel, the interference could be due to the previous symbol, while in single carrier systems, there is a similar interference due to several other symbols instead of only one previous symbol. The reason behind this problem is the symbol period is much shorter than the time span of the channel. The second problem is related to the subcarrier of a given OFDM symbol which is called Inter-carrier Interference. It is necessary to know how the OFDM system should deal with these two types of interference.

1.4.7 Intersymbol Interference

In the OFDM system, the data rate is reduced by the factor of N . Therefore, if there is a single-carrier system with a data rate equal to R symbol/second, the

OFDM system with N subcarrier has the data rate equal to R/N symbol/second. It gives the longer symbol period by the factor of N . Consequently, by choosing an appropriate number of subcarriers, it is possible to make the OFDM symbol longer than the time span of the channel. By this configuration, the distortion is limited to the first samples (according to the length of time span) in the OFDM symbol received at the receiver.

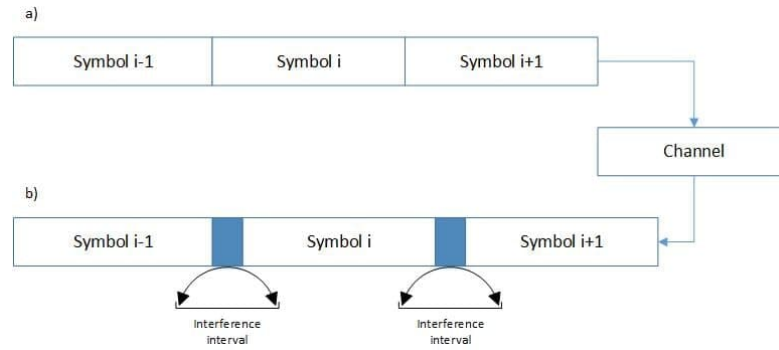


Figure 1.5: Intersymbol Interference (ISI). a) OFDM symbol frame structure at transmitter side. b) OFDM symbol frame structure at the receiver side.

Figure 1.5, depicted the interference interval. In ISI two symbols will overlap and causes distortion. Therefore, to minimize the effect of overlapping, the interference interval which is the guard interval is added between two transmitted frames. This method is called zero prefixes in which zero samples are added to the front of each symbol. The effect of the before transmitted frame will affect zero-padding portion of frames. Since the zero-padding portion does not contain any useful information, it is discarded to the receiver, and unaffected samples are used for demodulation of the signal transmission. By choosing the length of the guard interval properly such that it should be longer than the time span of the channel, the OFDM symbol itself will not be distorted and the effect of the intersymbol interference will vanish.

1.4.8 Intercarrier Interference

Notwithstanding that the zero-padding method represents a solution to eliminate the distortion due to intersymbol interference, it is not used in practical systems because it does not prevent an OFDM symbol from interfering with itself which is called intercarrier interference. Recall that in continuous time, convolution in the time domain is equivalent to multiplication in the frequency domain. In the case of discrete-time, this property is true only if the signals have an infinite length or if at least one of the signals is periodic over the range of the convolution. It is not possible to have the infinite-length OFDM symbol, however, it is possible to make

an OFDM periodic symbol.

In order to have the periodic OFDM symbol, it is necessary to replace the zero-padding portion of the symbol with a concept known as a cyclic prefix. The cyclic prefix replaces the zero-padding portion with the last samples of the OFDM symbol. This part should be greater than the time span of the channel. Similar to the zero-padding portion, this part is also redundant. Therefore, the cyclic prefix will be discarded at the receiver side.

With adding the cyclic prefix, the OFDM symbol now appears periodic. Consequently, the property of changing the convolution with multiplication from time-domain to frequency-domain is also valid for discrete-time and the effect of the channel becomes multiplicative.

On the receiver side, In a digital communication system, there are samples that have been convolved with the time-domain channel impulse response. Thus, the effect of the channel considers as a convolution. Nullification of the effects of the channel is done by applying another convolution at the receiver side by using the time-domain filter known as an equalizer. The equalizer has the length on the order of the time span of the channel. The equalizer processes symbols in order to adapt its response in an attempt to remove the effects of the channel.

In OFDM, the time domain signal is still convolved with the channel response. However, the data will be transformed back into the frequency domain by the FFT in the receiver. Due to the periodic nature of the cyclically extended OFDM symbol, the convolution in the time domain will be the multiplication in the frequency domain. Therefore, in frequency-domain, each subcarrier's symbol of the OFDM signal will be multiplied by the channel's frequency response of that specific subcarrier's frequency. The channel's frequency response is a complex number that each received subcarrier experiences as an amplitude and phase distortion.

In order to nullify the effect of the channel, it is possible to use an equalizer. For the simplest case in the absence of the noise, the equalizer is a filter that tries to apply the inverse of the channel's frequency response. There is a frequency domain and time domain equalizer. The former is much simpler than the latter and it consists of a single complex multiplication for each subcarrier.

Chapter 2

Channel Equalization

2.1 introduction

The evolution of the communication industry is mainly focused on the transmission of analog and digital signals over analog channels. Due to the increasing popularity of high-speed data transmissions, increasing spectrum efficiency on band-limited channels is unavoidable. Therefore, using the higher speed data transmission makes the channel more sensitive to disturbances. In order to compensate for the effect of the channel, we need to have an equalization scheme. Channel equalization is a method, using to reduce intersymbol interference. It is used to compensate for the effect of the channel. Figure 2.1 depicted the place of the equalizer block in the receiver. Generally, there are two broad categories for equalization. The first method is based on sequence estimation and the second one is based on filtering.

In the first kind of equalizer, instead of detecting each symbol separately, the data is detected considering a sequence. One of the optimal methods in this category is *maximum-likelihood sequence estimation* (MLSE). While MLSE provides the optimal performance but the price of this functionality is high implementation complexity.

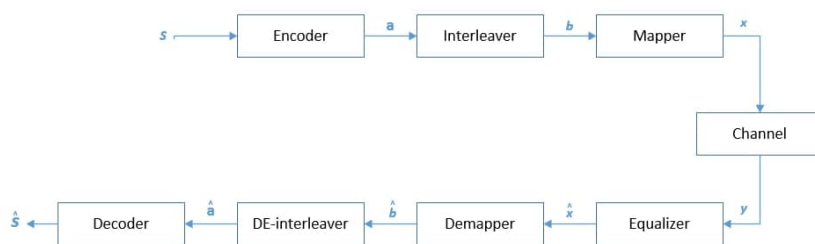


Figure 2.1: Transmitter and receiver and the equalization block

The second approach works based on applying the filter in order to decrease the channel impact on transmitted data. Therefore, the distortion of the channel will be compensated by finding an appropriate filter. Although this approach has a quite low implementation complexity, the algorithm is sub-optimal.

2.1.1 Sequence Estimated-base Equalization Method

Generally, for making the optimum decision, it is necessary to consider the entire sequence of received symbols, not just a few ones. The equalization would be sub-optimal if the it is performed based on considering the limited number of received symbols. We will see in next section, filter-based equalizer can provide a condition in which the equalizer cannot generate an optimal solution where the length of the channel is greater than the equalizer filter length.

Maximum likelihood sequence estimation (MLSE) is the principle that makes the optimal solution by considering the whole sequence. It determines the sequence of the symbols which has the most likely been transmitted [4]. The received signal at the receiver is as follow:

$$\mathbf{r}_i = \sum_{n=0}^L h_n c_{i-n} + n_i \quad (2.1)$$

where n_i is AWGN with variance σ_n^2 , L is the memory of the channel.

The joint pdf of the vector of received symbols \mathbf{r} , conditioned on the data vector \mathbf{c} and impulse response \mathbf{h} , is given by

$$p(\mathbf{r}|\mathbf{c}, \mathbf{h}) = \frac{1}{(2\pi\sigma_n^2)^{N/2}} \exp\left(-\frac{1}{2\sigma_n^2} \sum_{i=1}^N \left|r_i - \sum_{n=0}^L h_n c_{i-n}\right|^2\right) \quad (2.2)$$

The MLSE of \mathbf{c} maximizes $p(\mathbf{r}|\mathbf{c}, \mathbf{h})$ for a given \mathbf{h} that is correspond to minimizing

$$\sum_{i=1}^N \left|r_i - \sum_{n=0}^L h_n c_{i-n}\right|^2 \quad (2.3)$$

The complexity of equalization methods based on the exhaustive search for \mathbf{c} is very high especially in comparison with equalization based on filtering. This superior complexity provided an equalization of the signal with hundred of memory elements at a fraction of the computational cost of optimal equalizer [5].

In the MLSE principle, there is a possibility of considering the equalization process as a solution of the problem of estimating the state of the finite state machine or as an iterative process in which the path with the maximum weight in trellis is desired. In order to find the path with maximum weight, it is possible to use the Viterbi or brute-force method. Viterbi algorithm is an efficient recursive algorithm in which all possible input sequence is represented by a trellis.

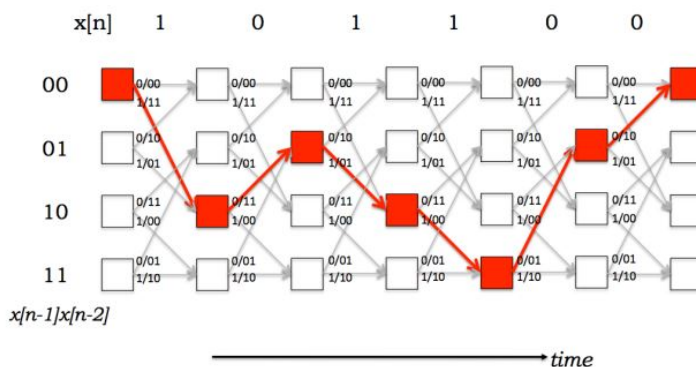


Figure 2.2: trellis diagram using in MLSE equalization

Figure 2.2 shows the diagram of a trellis. In order to use the Viterbi algorithm, we use two metrics: the Branch metric and the Path metric. The branch metric measures the distance between what is transmitted and received that is defined for each arc in the trellis. While the path metric is the value associated with the state in the trellis. In the Viterbi algorithm, the receiver can compute the path metric for a state/time pair incrementally using the path metrics of the previously computed state and the branch metric. It is possible to have unique paths for all 2^n possible input sequences by a trellis that extends for n sampling times. Although the Viterbi algorithm has a lower complexity in comparison with the brute-force method, the complexity of sequence-based equalizers is still very high compared with filter-based equalizers. Consequently, the MLSE equalization methods are not useful for real-time implementation purposes.

2.1.2 Filter-base Equalization Method

There are different equalization methods in the approach based on filtering. According to the type of filter used for equalization which can be one of the most important criteria, it is possible to consider the equalization method as *linear equalization* and *nonlinear equalization*. The difference between these two categories is the elements of the linear equalization is feedforward elements while in nonlinear equalization both feedforward and feedback elements can be used.

Another important criterion is the ability to adapt the equalization filter to change the channel condition. Considering this criterion, equalization algorithm either be *preset* or *adaptive*. Using the preset or adaptive methods depends on the behavior of the channel. If the channel is not changing during the transmission time, it only needs to compute the coefficient of the filter once. So, it is possible to use a filter with a preset coefficient. While the environment in which the channel condition is changing, the coefficients of the filter require to be updated over and

over by an adaptive algorithm during transmission time. In this kind of receiver, there is a training sequence in order to find the tap coefficients. This sequence will be sent by information periodically which is not carrying any information. Therefore it is totally wasted.

2.1.3 Linear equalization

A linear equalization is usually implemented by a finite impulse response filter [4]. Figure 2.3 depicted a linear equalizer that consists of a delayed line and a block to compute the weights of the tap coefficients. The input of the equalizer is the sequence x_i entering into the FIR filter of length L and each tap of filter has the specific weight which will be multiplied by that. Then sum all the values up and this value introduces the estimated output. After finding the estimated output, it will compare with the desired output and will compute the error. This is done in training state by training sequence which is known on the receiver. By computing the error, it is possible to update the weight. If there is a channel that is changing during transmission time, the weights should train from time to time. Therefore, the training sequence should exist periodically to update the tap coefficients. Consequently, it is possible to have another important criterion which is the ability to change the weights during transmission time and this can add the adaptation property to the equalizer. The equalization can be performed by different metrics that make us different kinds of equalizers. the next section described two equalizers with different metrics.

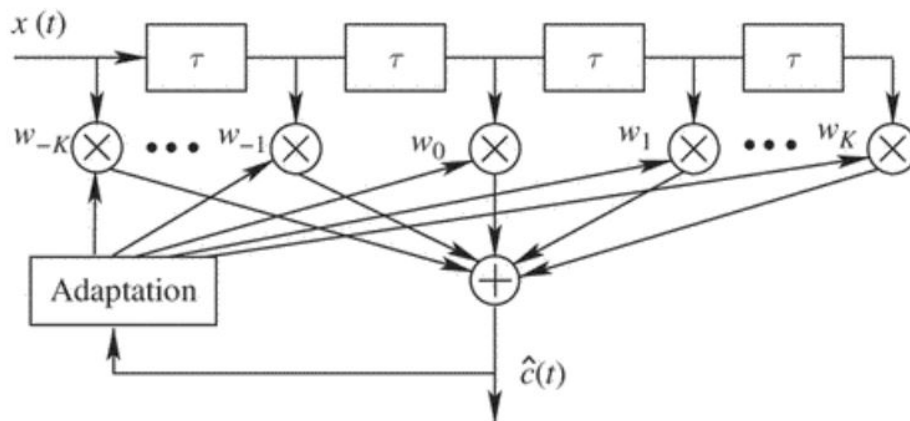


Figure 2.3: Block diagram of a linear equalizer made by the transversal FIR filter [4].

A. Zero-forcing Equalization

Zero-forcing equalizer tries to remove the ISI distortion by applying the inverse of the channel frequency response. Therefore, by applying the $H_c^{-1}(f)$, it is possible to have an ideal situation in which we can have a completely flat transfer function. It forces the ISI to zero at the sampling instant $t = kT$, $k = 0, 1, \dots$ [4]. The output of the ZF equalizer is as follow:

$$\mathbf{y}_k = d_k + n_k \quad k = 0, 1, \dots \quad (2.4)$$

where d_k is the desired symbol and n_k is the additive noise. At frequency in which the transfer function of the channel has a small value, the ZF equalizer enhances the noise of the channel, since it performed the inverse of the channel frequency response.

By applying the ZF equalizer to each sample at $t = mT$

$$\mathbf{d}(mT) = \sum_{i=-k}^k W_i x(mT - i\tau) \quad (2.5)$$

This equation is equal to 1 when $m = 0$ and is 0 when $m = \pm 1, \dots, \pm K$. This is the $2K + 1$ linear equation for the coefficients w_i of the ZF equalizer. In matrix form [4]

$$\mathbf{X}\mathbf{w} = d, \quad (2.6)$$

where $X_{ij} = s(iT - j\tau)$, $j = -K, -k + 1, \dots, K$, $w = (w_{-K}, \dots, w_k)^T$ and $d = (0, \dots, 0, 1, 0, \dots, 0)^T$. Then in ZF solution is

$$\mathbf{w} = \mathbf{X}^{-1}d. \quad (2.7)$$

B. MMSE Equalization

The ZF equalizer eliminates the ISI while it enhances the noise of the channel. Therefore it makes the BER performance undesirable. There is a better solution is known as MMSE equalization in which the tap coefficients are updated by minimizing the mean squared error criterion.

$$\min J = E[|c_k - z_k|^2] \quad (2.8)$$

where the z_k is the output of the equalizer. The optimum MMSE solution is given by

$$\mathbf{W}w_{opt} = (\mathbf{R}_{\mathbf{xx}}^T)^{-1}\mathbf{p}^T \quad (2.9)$$

where $\mathbf{w} = (w_{-L}, \dots, w_L)^T$, the correlation matrix of the received signal $\mathbf{R}_{\mathbf{xx}} = E[u_m u_m^H]$, $\mathbf{p} = E[u_m c_m^*]$, and $u_m = (x(mT + k\tau), x(mT - (-K + 1)\tau), \dots, x(mT - K\tau))^T$. Therefore

$$\mathbf{R}_{xx} = \frac{1}{2K + 1} \mathbf{X}^T \mathbf{X} + \sigma_0^2 \mathbf{I} \quad (2.10)$$

with σ_0^2 is the variance of the noise at the receiver. The $\mathbf{R}_{\mathbf{xx}}$ and \mathbf{p} are given by

$$R_{xx}(i, j) = R_{xx}(i - j) = E[x(mT - i\tau)x^*(mT - j\tau)] + \delta_{ij}\sigma_0^2 \quad (2.11)$$

for $i, j = -K, -K + 1, \dots, 0, \dots, K$, where $E[\cdot]$ is over all values of m , and δ_{ij} is the Krocknecker delta function. This solution is known as the Wiener solution. The MMSE is given by [4]

$$\mathbf{J}_{min} = 1 - \mathbf{p} \mathbf{R}_{\mathbf{xx}}^{-1} \mathbf{p}^T \quad (2.12)$$

2.1.4 Adaptive Algorithms

To generate the desired output and equalizing in an optimum manner, it is necessary to have the well-known channel matrix at the receiver. According to [6], the equalizer works properly only if there is a priori information about the statistics of the data which should be matched with the statistical characteristic of the input data. As a solution, it is possible to design an equalizer with an adaptive algorithm in which there is a recursive algorithm in order to work properly in an environment where the complete knowledge of the relevant characteristics does not existed or they are changing during the time. The purpose of an adaptive equalizer is to generate an output such that the cascade of the equalizer and the channel provides an approximation of an ideal transmission medium [7]. An equalizer with an adaptive algorithm should be adapted to the time-varying properties of the channel automatically by self-adjusts its transfer function regarding a specific optimal algorithm. Figure 2.4 shows a diagram of a channel equalization system.

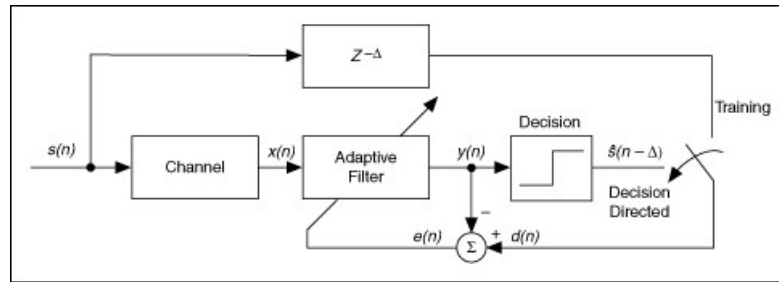


Figure 2.4: Block diagram of equalizer considering adaptive algorithm block [8].

According to the previous figure, $s(n)$ is the input of the system and $x(n)$ is the distorted version of the signal. To compensate the distortion of the signal, the adaptive equalizer should perform the following modes [8]:

- Training mode: To determine the proper tap coefficients, it is necessary to perform this step. This is done by sending a delayed version of the same input $d(n)$ to the adaptive filter. The error $e(n)$ is computed by taking the difference between the output of the equalizer $y(n)$ and $d(n)$. The equalizer adjusts the tap coefficients to minimize this error. Convergence power of the error makes the $y(n)$ identical to $d(n)$ and then the filter coefficient can be used to compensate the channel distortion.
- Decision mode: After finding the appropriate tap coefficient, it is possible to use the equalizer to estimate the input signal.

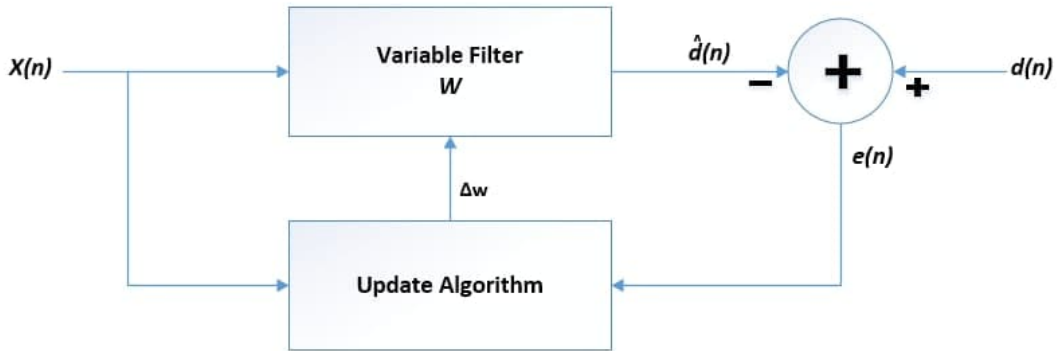


Figure 2.5: Adaptive filter

Figure 2.5 shows the diagram of the adaptive algorithm. It can be assumed that the input signal is the summation of the desired signal $d(n)$ and interfering noise $v(n)$.

$$\mathbf{x}(n) = d(n) + v(n) \quad (2.13)$$

Since the structure of the variable filter is Finite Impulse Response (FIR), the impulse response is equal to the filter coefficients [9]

$$\mathbf{W}_n = [W_n(0), W_n(1), \dots, W_n(P)]^T$$

where the P is the order of the filter.

The error signal is defined as the difference between desired signal and the estimated one

$$\mathbf{e}(n) = d(n) - \hat{d}(n) \quad (2.14)$$

The $\hat{d}(n)$ is computed by convolving the input signal and the impulse response. in vector notation:

$$\hat{\mathbf{d}}(n) = \mathbf{W}_n * \mathbf{x}(n) \quad (2.15)$$

where

$$\mathbf{x}(n) = [x(n), x(n-1), \dots, x(n-P)]^T$$

is the vector of the input signal. The filter updates the tap coefficient at each time instant

$$\mathbf{W}_{n+1} = \mathbf{W}_n + \Delta W_n \quad (2.16)$$

where ΔW_n is the updating factor for the tap coefficients which is generated by the adaptive algorithm based on the error signal. For this purpose, there are two main algorithms used in the adaptive algorithm. First one is the least mean square (LMS) and the second is the recursive least square (RLS) method.

A. Least Mean Squares Algorithm (LMS)

A more robust adaptive algorithm is used to mimic the desired filter by finding the weights of the taps providing the least mean squares of the error signal which is defined as the difference between desired and the actual signal. It is actually a stochastic gradient descent method that is adapted based on the error at the current time. Figure 2.6 shows an adaptive filter based on LMS algorithm [8].

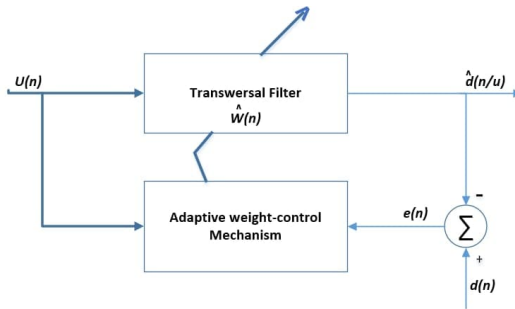


Figure 2.6: Block diagram of an adaptive transversal filter with LMS algorithm.

The algorithm starts by considering small tap coefficients (zero in most cases) and at each step by applying the stochastic gradient algorithm of mean square error, the tap coefficients will be updated.

The LMS algorithm consists of two steps. The first step is computing the error

$$\mathbf{e}(n) = d(n) - y(n) \quad (2.17)$$

where $y(n)$ is the desired response at time n . the error is the difference between desired and actual value. In the second step, the tap coefficients will be updated by summing the previous weight with the error multiplied by a step size.

$$\hat{\mathbf{W}}(n+1) = \hat{\mathbf{W}}(n) + \alpha \mathbf{e}^*(n) \quad (2.18)$$

where the α is the step size that is a design parameter and specifies the convergence step in a stochastic gradient algorithm. if the step size is a large value the convergence could be faster but it may never convergence.

As it is shown in Figure 2.6, these two processes are made by a feedback loop. The filtering process is done by the transversal filter and then there is an algorithm to perform the adaptive process.

Despite, LMS algorithms converge slowly and work well if the channel is not changing fast, but it is a robust and most well-known adaptive algorithm and according to the computational simplicity, There are many application use this algorithm in order to have an adaptive equalizer.

B. Recursive Least Square Algorithm (RLS)

The Recursive least square (RLS) algorithm is an adaptive algorithm that finds the weights of the taps by minimizing the least squares cost function which is related to the input signal. There are some differences between this algorithm and LMS such as considering the input signals as a deterministic signal while in LMS we assume the input signal is stochastic. The RLS algorithm prepares fast convergence compared with the LMS algorithm while the cost of this advantage is higher complexity and poor tracking ability when we have a channel that is changing during the time [9]. The procedure of the algorithm is the same as the LMS algorithm which is shown in Figure 2.6, except that in RLS it is possible to provide a tracking rate sufficient for the selective channel.

2.2 Channel Shortening

The channel shortening (CS) is a well-known concept in which the linear vector channels can transfer into a "shortened" version. This is done for reducing complexity in demodulation and improving data transmission performance [10]. Moreover, this technique is an efficient method to provide a smaller equivalent channel length to the demodulator and it can also be used in order to have a shorter guard interval in the systems like OFDM. Therefore, it is possible to have better spectral efficiency.

The addition of CP in OFDM broadcasting systems reduces the throughput of the channel as it transports unneeded data. The channel shortening is an alternative solution for the OFDM receivers with a long CP length to deal with multi paths environment. Channel shortening was first proposed in single carrier systems [11] to reduce the complexity of the trellis detector in ML receiver. The channel shortening principle was also used in multi carrier system [12] as a time-domain equalizer to make the equivalent channel response length smaller than the CP thus allowing single tap equalization in the frequency domain [10].

The initial idea of channel shortening is using the filter for the received signal which leads to having a shorter effective channel than the original one. Then, by applying the Viterbi Algorithm, it is possible to detect the samples with affordable complexity. Consequently, channel shortening is the combination of filter-based equalization and sequence-based equalization method. Afterward, the channel shortening idea has been developed and optimized from a various perspectives such as minimum-phase filtering, Kalman-filtering, minimum mean-square error (MMSE), etc.

There are solutions in channel shortening which is [13] suggested the usage of per tone equalizer (PTEQ) for ADSL applications. They assigned a specific T-Taps equalizer for each carrier separately to optimize the SNR for each carrier. These techniques were based on the minimization of mean square error and this metric does not provide in general the highest throughput. In the next section, the channel shortening method in [13] is described.

2.2.1 Optimal channel shortening

The received signal can be represented as a complex-valued discrete-time model as follows:

$$\mathbf{y} = \tilde{\mathbf{H}}\mathbf{x} + \mathbf{w}', \quad (2.19)$$

where \mathbf{y} is the received signal, $\tilde{\mathbf{H}}$ is ISI/ICI channel matrix of dimension $T \times T$ which is perfectly known to receiver, \mathbf{x} is the input data which is circularly-symmetric complex Gaussian distributed and \mathbf{w}' Additive Gaussian Noise with variance N_0 . The channel matrix $\tilde{\mathbf{H}}$ includes IFFT, TDL channel (h) and FFT. The absolute limit of achievable rate (I_R) over TDL channel (h) with length L is

$$I_R = \log_2 \left(1 + \frac{\|h\|^2}{N_0} \right), \quad (2.20)$$

where N_0 is the noise power spectral density. The Equation 2.20 assumes uniform power allocation over all carrier. Now based on the approach in [14], the optimal receiver is characterized by an optimal $\tilde{\mathbf{H}}^r$ filter given by:

$$\tilde{\mathbf{H}}^r = \left[\tilde{\mathbf{H}}\tilde{\mathbf{H}}^\dagger + N_0\mathbf{I} \right]^{-1} \tilde{\mathbf{H}}^\dagger(\tilde{\mathbf{G}}^r + \mathbf{I}), \quad (2.21)$$

which is a standard MMSE/Wiener filter compensated by trellis processor represented by matrix $\tilde{\mathbf{G}}^r$. The $\tilde{\mathbf{G}}^r$ is a suitably designed matrix that satisfy the following property:

$$(G^r)_{mn} = 0 \quad \text{if} \quad |m - n| > \nu,$$

where $(G^r)_{mn}$ define elements of matrix $\tilde{\mathbf{G}}^r$ and ν denotes memory of reduced trellis memory.

According to [14] the lower bound of theoretical achievable rate of optimal filter $\tilde{\mathbf{H}}^r$ becomes:

$$\begin{aligned} I_{LB}(\nu) &= \log \left(\det(\mathbf{I} + \tilde{\mathbf{G}}^r) \right) \\ &+ \text{Tr} \left\{ [\tilde{\mathbf{G}}^r + \mathbf{I}] \tilde{\mathbf{H}}^r [\tilde{\mathbf{H}} \tilde{\mathbf{H}}^\dagger + \mathbf{N}_0 \mathbf{I}]^{-1} \tilde{\mathbf{H}} \right\} \\ &- \text{Tr} \left\{ \tilde{\mathbf{G}}^r \right\}, \end{aligned} \quad (2.22)$$

where $I_{LB}(\nu) < I_R$.

We can define the following throughput efficiency metric as performance metric of channel shortening receiver:

$$T_E(\nu) = \frac{I_{LB}(\nu)}{I_R} \times \frac{N}{N + P}, \quad (2.23)$$

with $0 < T_E \leq 1$. Notice that we included in the definition the correction coefficient $\frac{N}{N+P}$ due to insertion of CP.

In the next chapter, we will see designing a 2-D MMSE equalizer based on channel shortening principle that has been obtained along the procedure outlined in [13], provided higher throughput efficiency. While these promising results are based on the very strong assumption of perfect channel knowledge at the receiver. In practice, it is well-known that channel estimation is a very crucial function for receiver performances, especially in a mobile environment. To address this problem, it is possible to design a low complexity and adaptive 2D channel equalizer which can acquire and track the ISI/ICI channel.

2.3 Implementation of 2-D Adaptive MMSE Equalizer for OFDM Systems With Insufficient Cyclic Prefix

As is mentioned previously, in OFDM systems, thanks to using the small subcarrier spacing technique, we can carry data on several parallel data streams which brings the spectral efficiency. In order to be resistant to multipath interference, it is necessary to use a portion of the transmission time for the cyclic prefix (CP) which

must be greater than or equal to the delay spread of the channel. This delay spread can become significant especially for long range transmission, Therefore, having sufficient CP leads to degradation in data rates and efficiency. Insufficient CP in OFDM transmission causes ISI and ICI and we have time and frequency selectivity. In this case, the single-tap equalizer cannot reconstruct the original OFDM symbol. As it is mentioned, an alternative solution is using the channel shortening principle. To combat the time and frequency selectivity we need to design an equalizer that is able to compensate the effect of the channel in two dimensions that must be adaptive.

Our aim is to design and implements a low-complex 2-D adaptive equalization that is able to equalize in two dimensions. The input of the equalizer can be in 2-D as is shown by Figure 2.7. The size of the input is related to the number of subcarriers (N) and the memory of the channel (L).

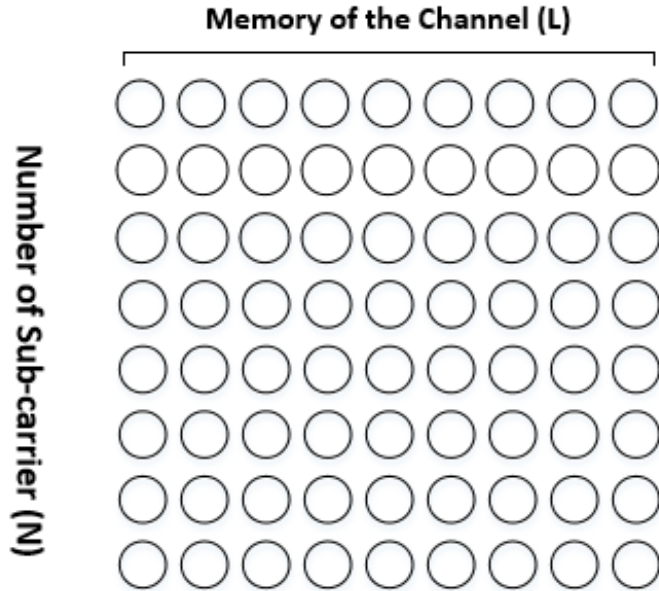


Figure 2.7: From of the input of the 2-D equalizer

Figure 2.8 shows the block diagram of a 2-D adaptive MMSE equalizer based on the 2-D transversal filter. The input of the equalizer is the symbols of different subcarriers and the number of taps is chosen based on the memory of the channel. The process is done similarly to what we have in the MMSE adaptive equalizer. At each iteration, the error is computed according to Equation 2.17 by taking the

difference between the output of the equalizer (y) and the desired signal that is the delayed version of the input (d_{n-D}). Then the error is used in order to update the tap coefficients by using Equation 2.18.

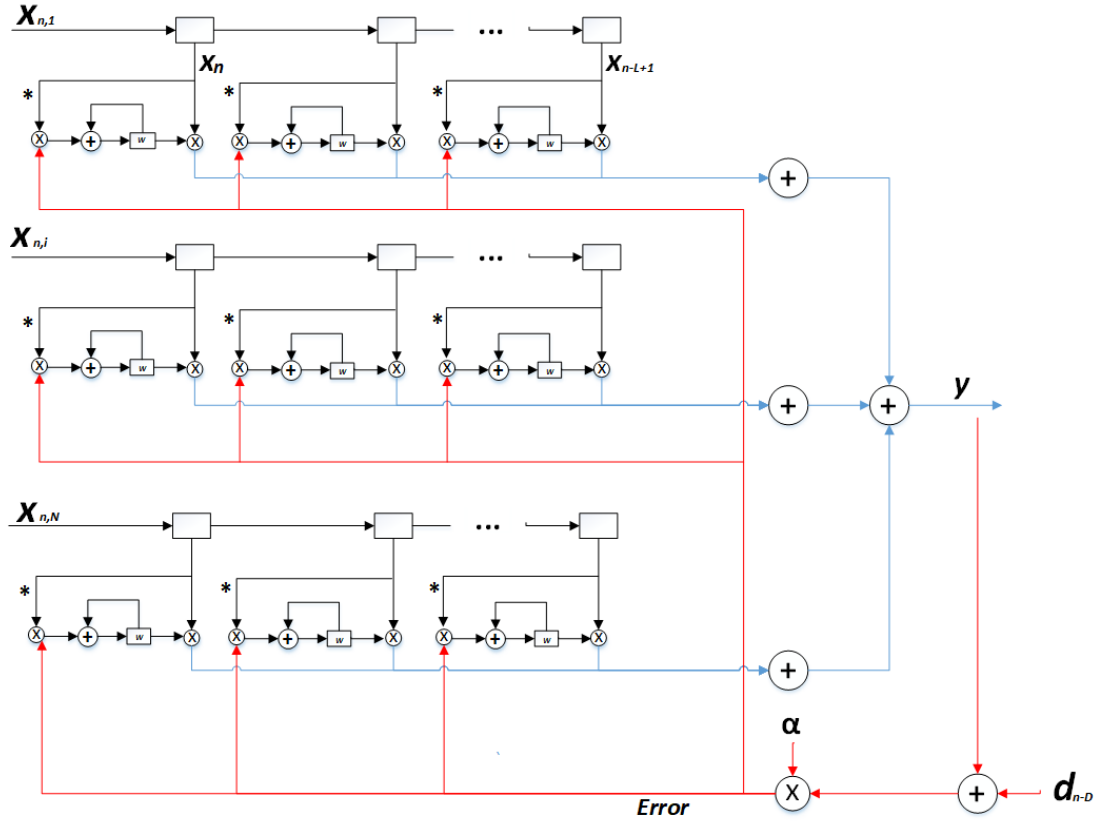


Figure 2.8: block diagram of a 2-D equalizer

The most important criterion in designing the equalizer is the complexity of computation. As is illustrated by Figure 2.8, increasing the number of active taps leads to having more computational complexity. Therefore, the complexity is changed by the size of the filter that is equal to the number of the sub-carriers (N) and the memory of the channel (L).

The algorithm is designed such that it is possible to consider a window for selecting the Active taps in different shapes and different sizes. Actually, the shape of the window is the important parameter that we want to consider base on the norm (L_p) of the vector. Figure 2.9 shows the p-norms of the unit vector. It is a way that makes the implementation of the equalizer more flexible in order to have a good performance with resealable complexity. By using different geometric shapes for selecting the active taps and comparing them with each other, it is possible to

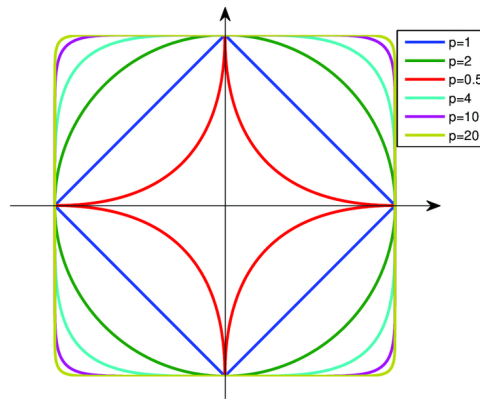


Figure 2.9: p-norms of the unit vector [15].

choose a shape with more relevant taps with the same complexity to perform the equalization.

As an example, Figure 2.10 shows the shape of the active taps with Rectangular, Cross and Rhombic shapes.

The algorithm of implementation is based on LMS adaptive algorithm. In the first step, it is important to make the equalizer flexible in order to choose the shape and the size of the window. The equalizer makes the window based on the shape and size. Then, the active taps for each element are selected and used for the equalization process. The equalization process is similar to the process that is explained in chapter 2. Calculation of the error and use it in order to update the weight of the taps. There are different criteria belong either to the equalizer like learning rate or to the system like delay spread, SNR, etc, that need adjustment to make an optimal equalization. As a consequence, there are many possibilities that should be considered to design a low complex equalizer with reasonable performance.

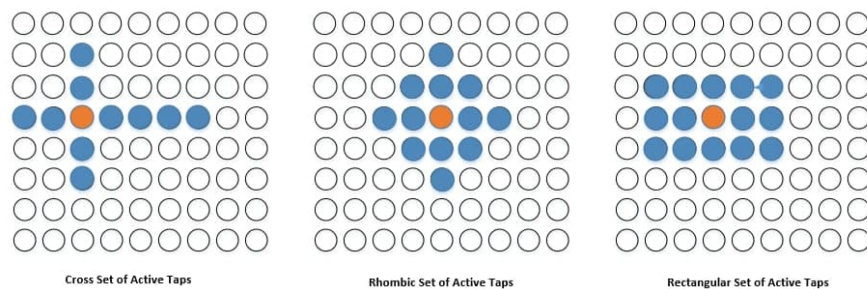


Figure 2.10: Different shapes for active taps

In this chapter, we start from the framework developed in [14] to derive optimal receiver structures satisfying broadcast transmission requirements using 5G NR numerologies. Then, the complete system model for broadcasting transmission in an SFN network will be introduced. In particular, the steps describing the construction of an equivalent channel matrix are illustrated. Afterward, the channel shortening method in [14] with simulation and its result is illustrated. And finally, another channel shortening technique is represented which takes advantage of shorter equivalent channel response length by design and implementing the 2-D MMSE equalization method.

In the next chapter, first, we derive the optimal receiver structure satisfying broadcast transmission requirements using 5G NR by developing [14]. Then, the performance of the system with the channel shortening technique is represented which takes advantage of shorter equivalent channel response length by design and implementing the 2-D MMSE equalization method. In the last part, we illustrate the results of the adaptive 2-D MMSE equalizer as well as the comparison of the results in the same and different complexity. Finally, comparing the performance of the adaptive equalizer with the optimal value which is obtained by optimal channel shortening filter is considered.

Chapter 3

Single Frequency Network Broadcasting with 5G NR Numerology

3.1 Introduction

As it is explained in previous chapter, in a Single Frequency Network (SFN), a signal is transmitted simultaneously through multiple stations over the same frequency channel. Several useful signals are available to the receiver either from multi path echoes or from different transmitters. The receiver in SFN must be able to overcome multi path conditions and its performances are strongly affected by the performance of channel equalizer.

In an Orthogonal Frequency Division Multiplexing (OFDM) system by adding a Cyclic Prefix (CP) between the OFDM symbols which is at least the size of the Channel Impulse Response (CIR), the non-constructive combination of signals in the receiver can be prevented and a simple receiver structure can be obtained to equalize the channel with only one complex multiplication for each carrier.

The DVB-T2 (2nd Generation Digital Video Broadcasting Terrestrial) [16] as well as the ATSC 3.0 (Advanced Television Systems Committee) [17] standards allow for large inter-site distances covering up to hundreds of kilometers (e.g. 60 km - CP duration of 200 μ s - or 120 km - CP duration of 400 μ s). In parallel, the Third Generation Partnership Project (3GPP) introduced 5G New Radio (5G NR) air interface from Release 15 [1] offering a more flexible and scalable design than LTE, in order to satisfy a wider range of use cases requirements, frequency bands and deployment options.

However, 5G NR only supports user-specific uni-cast transmissions. i.e. transmission modes and core functionality not complying with broadcaster's requirements. A multi-cast mode is currently under development in 3GPP Rel-17 Multimedia Broadcast Service (MBS), but it is limited to supporting general multi-cast and broadcast communication services (e.g. transparent IPv4/IPv6 multi-cast delivery, IPTV, IoT applications, V2X applications, public safety) relevant for distribution over 5G mobile networks. Indeed, 5G NR air interface standardized up to now, is not suitable for delivering media services over stand-alone Broadcast Downlink Network Only, employing large SFN areas in a Free-to-Air reception, and receive-only device [1].

As it is explained, the addition of CP in OFDM broadcasting systems reduces the throughput of the channel as it transports unneeded data. The channel shortening is an alternative solution for OFDM receiver with long CP length to deal with multi paths environment. Channel shortening was first proposed in single carrier systems [11] to reduce complexity of trellis detector in ML receiver. The channel shortening principle was also used in multi carrier system [12] as a time domain equalizer to make the equivalent channel response length smaller than the CP thus allowing single tap equalization in the frequency domain. Section 2.2 is described the concept of channel shortening as well as the principle of the optimal channel shortening which is suggested by [14].

In this chapter, we start the complete system model for broadcasting transmission in an SFN network will be introduced. In particular, the steps describing the construction of equivalent channel matrix are illustrated. Then, another channel shortening technique is represented which is take advantage of shorter equivalent channel response length by design and implementing the 2-D MMSE equalization method. And finally, the result of designing a low complexity and adaptive 2-D channel equalizer will be considered which can acquire and track the ISI/ICI channel also in highly mobile environments.

3.2 SFN Network System for Broadcasting Transmission

The system model is represented in Figure 3.1. N parallel inputs \mathbf{x} are mapped from the frequency domain to the time domain by means of an Inverse Fast Fourier Transform (IFFT) and CP insertion of size P . The OFDM symbol, of length $N + P$ is transmitted over the physical channel, modeled as a Tapped Delay Line (TDL) 5G channel model [18].

The TDL channel model can characterize a SFN, where all the transmitters use the same frequency and signals copies can reach user from different transmitters and possibly scatterers at the same time. In this case the ISD characterizing the

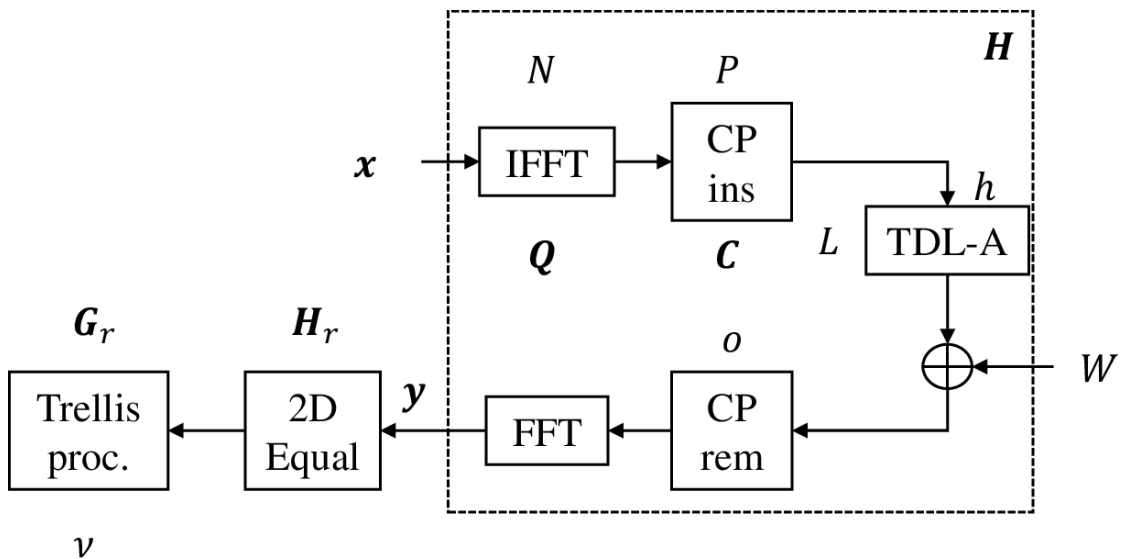


Figure 3.1: System Model

SFN is modeled with a proper Delay Spread (DS) of the TDL channel model. Two type of channels for TDL model are defined, the TDL-A channel profile with Non Line of Sight (NLOS) for handheld/mobile reception environments, and the TDL-E channel profile with Line Of Sight (LOS) for rooftop reception.

Table 3.1 is reported the model parameters of 4 SFN networks scenarios with different ISD and transmitted power. The 4 scenarios cover some possible configurations for terrestrial networks: High Power High Tower (HPHT) and Medium Power Medium Tower (MPMT) typically based on a limited number of transmitters with large antenna heights and Effective Radiated Power (ERP) values in the range of some kW to many tens of kW. Low Power Low Tower (LPLT) architecture is characterized by a dense network of transmitters, with rather low power levels and antenna heights. For each SFN network we report the delay spread derived from system level simulation to be used in the two TDL channel profiles [18].

Parameter	LPLT	MPMT	HPHT1	HPHT2
ISD [km]	15	50	125	173.2
Transmitted power [dBm]	46	60	70	70
LOS DS [μ s]	16	35	45	70
NLOS DS [μ s]	20	40	50	75

Table 3.1: Different SFN networks and correspondent Delay Spread (DS) in LOS (TDL-E) and NLOS (TDL-A) channel models.

We consider a TDL channel with channel impulse response (h) with length L , which is known to the receiver. In our setting the length of the impulse response of the channel L can be much larger than an OFDM symbol. So we derive a matrix representation of the system shown in Figure 3.1 as follows.

First define the following matrices, representing the block processing at TX and RX side:

IFFT: passing the input in order to transform to time domain from frequency domain.

$$\mathbf{Q}_{ij}^* = \frac{1}{\sqrt{N}} e^{j2\pi \frac{i \cdot j}{N}} \quad \forall i, j \in [0, N - 1]$$

CP prefix insertion:

$$\mathbf{C}_I = \begin{bmatrix} \mathbf{0}_{N-P} & \mathbf{I}_P \\ & \mathbf{I}_N \end{bmatrix},$$

where \mathbf{I}_N is the identity matrix of size N , and $\mathbf{0}_{N-P}$ is a zero matrix with P rows and $N - P$ columns.

CP removal:

$$\mathbf{C}_R^{(o)} = \text{cshift}_o \begin{bmatrix} \mathbf{I}_N & \mathbf{0}_P \end{bmatrix},$$

where “cshift _{o} ” accounts for a possible circular shift of the columns of the matrix, controlled the parameter o .

FFT:

$$\mathbf{Q}_{ij} = \frac{1}{\sqrt{N}} e^{-j2\pi \frac{i \cdot j}{N}}.$$

We then and use the conventional infinite Toeplitz matrix,

$$\tilde{\mathbf{H}}' = \text{Toep}_\infty[h_{L-1}, h_{L-2}, h_0],$$

to represent the effect of the channel linear convolution, and introduce the following block diagonal infinite matrices

$$\begin{aligned} \tilde{\mathbf{Q}}^* &\triangleq \text{Toep}_\infty[\mathbf{C}_I \mathbf{Q}^*] \\ \tilde{\mathbf{Q}} &\triangleq \text{Toep}_\infty[\mathbf{Q} \mathbf{C}_R^{(o)}], \end{aligned}$$

to represent TX and RX OFDM block processing. The notation $\text{Toep}_\infty(\mathbf{M}_1, \dots, \mathbf{M}_N)$ represents the infinite (block) Toeplitz matrix with (block) diagonals $\mathbf{M}_1, \dots, \mathbf{M}_N$. The output sequence \mathbf{y} can now be written as

$$\mathbf{y} = \overbrace{\tilde{\mathbf{Q}} \tilde{\mathbf{H}}' \tilde{\mathbf{Q}}^*}^{\tilde{\mathbf{H}}} \mathbf{x} + \mathbf{w}'$$

The OFDM processing then transforms the stationary channel in the time domain into a cyclo-stationary channel in the Finite Fourier Transform domain. The structure of channel matrix $\tilde{\mathbf{H}}$ becomes

$$\tilde{\mathbf{H}} = \text{Toep}_{\infty}(\mathbf{H}_{J-1}, \dots, \mathbf{H}_0)$$

where $J = \lceil \frac{L}{N+P} \rceil$, and \mathbf{H}_i are $N \times N$ matrices, substituting the original samples of the time domain impulse response h_i in \mathbf{H}' . Notice that this representation depends on the choice of the position of the CP removal offset o .

The introduced notation allows to represent OFDM systems in the general case where the length of the impulse response of the channel L take any value, even larger than P and N . In the special case, where $L < P$, corresponding to the usual setting for OFDM systems, the input-output relationship boils down to

$$\tilde{\mathbf{H}} = \text{Toep}_{\infty}(\mathbf{D}_0),$$

where \mathbf{D}_0 is a diagonal matrix carrying the FFT of the channel impulse response.

The derived input-output relationships can be now casted in the general model introduced in [14] to derive the optimal receiver based on channel shortening.

3.3 optimal channel shortening performance

The principle of the optimal channel shortening is described in 2.2.1. Based on the Equation 2.23, we can define the throughput efficiency metric as performance metric of the channel shortening receiver. In Figure 3.2 we report the $T_E(\nu)$ versus ν for different 5G NR numerologies and HPHT1 NLOS channel scenario of Table 3.1. All plots show increasing the performance with ν . In particular for $\mu = 0$ (15 kHz) we notice that the improvement obtained by increasing ν is marginal and the system reach rapidly the ultimate limit corresponding to CP overhead, that is 6% of 5G NR. So the solution with $\nu = \mu = 0$, corresponding to absence of trellis processor is very promising. This receiver can be constructed by simple 2D-MMSE equalizer without adding complexity of trellis processor.

On the other hand, a full complexity detector can be obtained by setting $\nu = T - 1$ and the optimal theoretical achievable rate becomes $I_{LB}(\nu) = I_R$. As previously mentioned the design of optimal delay offset is crucial for the final performance as it affects the structure of $\tilde{\mathbf{H}}^r$. In all reported performance this parameter was preliminary optimised by maximising the energy of received signal after cyclic prefix removal.

3.3.1 Simulation and result

According to the Equation 2.21, the performance of optimal $\tilde{\mathbf{H}}^r$ filter is presented. The TDL-A channel profile with delay spreads in Table 3.1 is used for evaluating

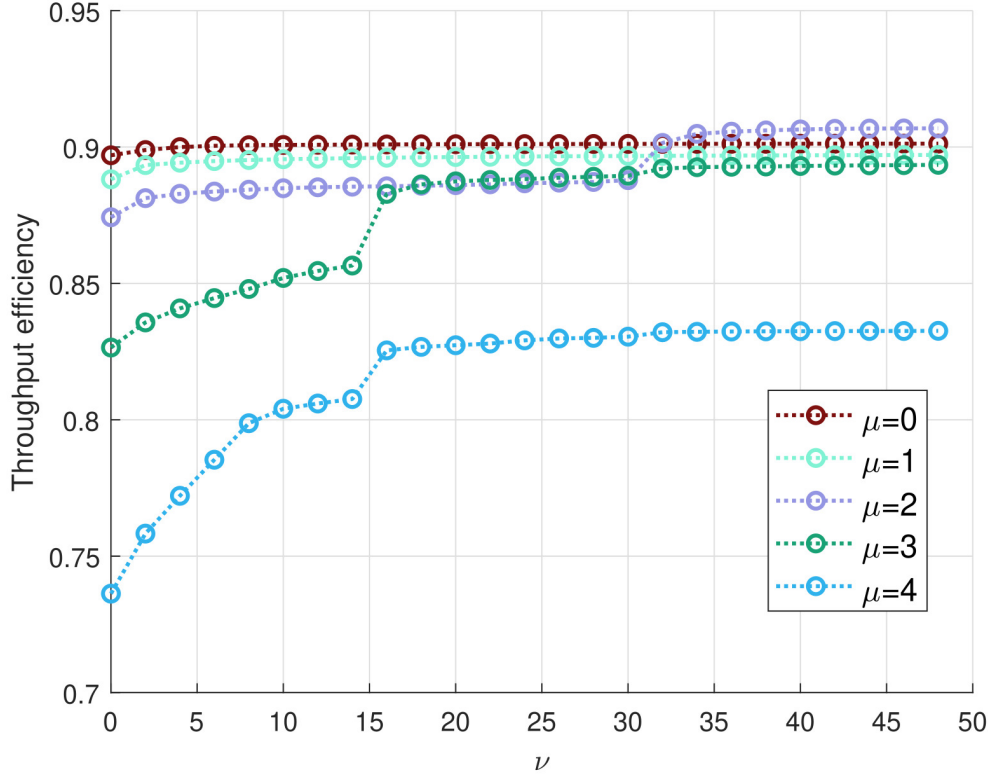


Figure 3.2: Throughput efficiency versus ν for 5G NR numerologies with fixed SNR=5dB and $SCS = 2^\mu \times 15\text{kHz}$

SFNs networks. The bandwidth used in all tests is 9.6 MHz. The velocity of receiver is equal to zero. The channel is assumed to be known at the receiver. The time synchronization and computation of optimal offset is performed as described previously.

3.3.2 Theoretical and Pragmatic achievable rate by $\tilde{\mathbf{H}}^r$ channel equalizer

In Figure 3.3 we report the throughput efficiency (Equation 2.23) of the filter $\tilde{\mathbf{H}}^r$ for $\nu = 0, 7$ and Gaussian inputs with $50\mu\text{s}$ delay spread. The standard 5G NR numerologies with normal CPs length (1/15 of useful signal) is used. These numerologies are given by:

$$SCS(\mu) = 15\text{kHz} \times 2^\mu \quad \mu = 0, \dots, 4,$$

For each of these numerologies and the $DS=15\mu s$, the maximum value for J is 7, 14, 28, 55 and 109 OFDM symbols, respectively. The case $\mu = 0$ shows the higher throughput efficiency for any signal to noise ratio, while the throughput efficiency decreases using larger 5G NR numerologies (e.g. $\mu = 4$). The cases with $\nu = 0$ (no trellis processor) and $\nu = 7$ provide similar T_E for small 5G NR numerologies ($\mu = 0,1,2$). On the other hand using trellis processing ($\nu = 7$) can provide significant gains for higher numerologies, especially at high signal to noise ratio.

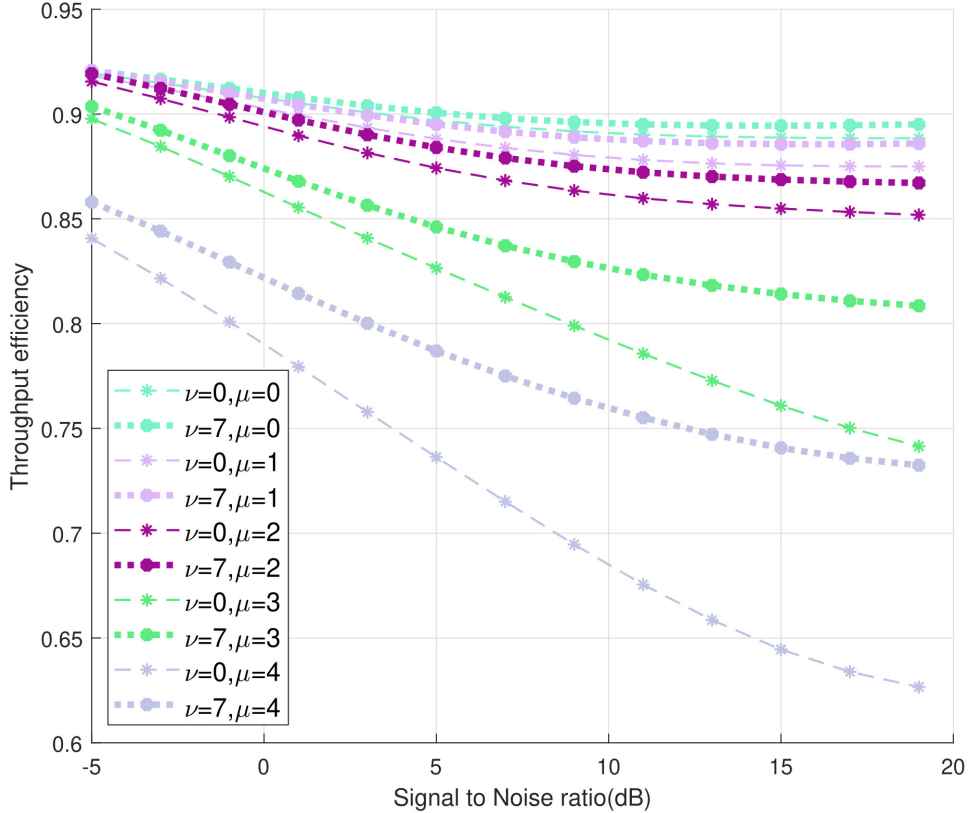


Figure 3.3: Throughput efficiency T_E versus receiver complexity (ν) for 5G NR numerologies: TDL-A $DS=50\mu s$ (HPHT1, NLOS, 125km ISD)

In Figure 3.4 we fixed the SNR to 5dB and reported the throughput efficiencies versus the sub-carrier spacing for the five 5G NR numerologies, two non-standard smaller carrier spacing (0.37, 2.5 kHz) and the single carrier case (9600 kHz), with $\nu = 0,7$. The CP overhead of the first two non-standard cases is the one specifically designed to allow to deal with large delay spread and with a single tap equalization.

The CP overhead is $\frac{1}{9}$ for 0.37 kHz and $\frac{1}{4}$ for 2.5 kHz. On the other hand no CP overhead is associated to the single carrier case.

For $\nu = 0$ (blue line), the best solution is with 15 kHz and provide almost 90% of T_E . For 5G NR carrier spacing around 6% of T_E loss is due to insertion of CP overhead and the remaining is associated to receiver loss. Smaller carrier spacing (0.37, 0.25 kHz) provide around 90% and 79% T_E . This loss is almost totally associated to the larger CP overhead associated to them. Notice that with $\nu = 0$ the 15 kHz also outperforms the single carrier case. This can be a motivation for using multi carrier OFDM system with 2D-MMSE $\tilde{\mathbf{H}}^r$ filter for broadcasting in a SFN network.

The single carrier on the other hand performs better by increasing receiver complexity ($\nu = 7$). In fact we can expect that by increasing ν , the T_E converge to the CP correction term in Equation (2.23) (see Figure 3.3), which is 1 in this case.

Based on results in Figure 3.4, 5G NR numerology with 15 kHz with a properly designed 2D-MMSE equalizer ($\nu = 0$) can be a competitive alternative to the 0.37 kHz carrier spacing (3000 μ s OFDM symbol length) and the need to use trellis processor ($\nu > 0$) is not required.

Previous bounds were obtained assuming an optimal Gaussian input distribution. A more accurate prediction of the system performance can be obtained by computing the mutual information associated to the typical BICM receiver structure. This performance metric, usually referred to as the “pragmatic” capacity, includes the losses due the adoption of a particular constellation and those due to the marginalization to the bit LLR that is performed in the receiver before the channel decoder.

The pragmatic capacities for the practical modulations QPSK (nbits=2), 16QAM (nbits=4) and 64QAM (nbits=6) using 15 kHz and 0.37 kHz carrier spacing are shown in Figure 3.5. For 15 kHz, we considered both the 2D-MMSE (solid line) and the single tap equalizer (dash-dotted line) receiver, for 0.37 kHz we considered only the single tap receiver (dashed line). As a reference, we reported the theoretical information lower bound (I_{LB}) using 15 kHz carrier spacing with Gaussian inputs.

The 2D-MMSE equalizer with 15 kHz carrier spacing and single tap equalizer with 0.37 kHz carrier spacing, provide similar pragmatic capacities, with the first slightly better. Increasing the signal to noise ratio the pragmatic capacity of 2D-MMSE and single tap equalizer (0.37 kHz) converges as expected to the modulation efficiency (2, 4 and 6 bits). In low signal to noise ratio the pragmatic capacity provided by 2D-MMSE is close to the theoretical limit with Gaussian inputs (I_{LB}). The single tap equalizer with 15 kHz carrier spacing on the other hand can not compensate ISI/ICI interference and increasing the signal to noise ratio can not improve achievable information rate above one. Base on result in Figure 3.5 the 15 kHz with 2D-MMSE equalizer has similar or even better performance w.r.t. single tap equalizer with long CP length (0.37 kHz carrier spacing).

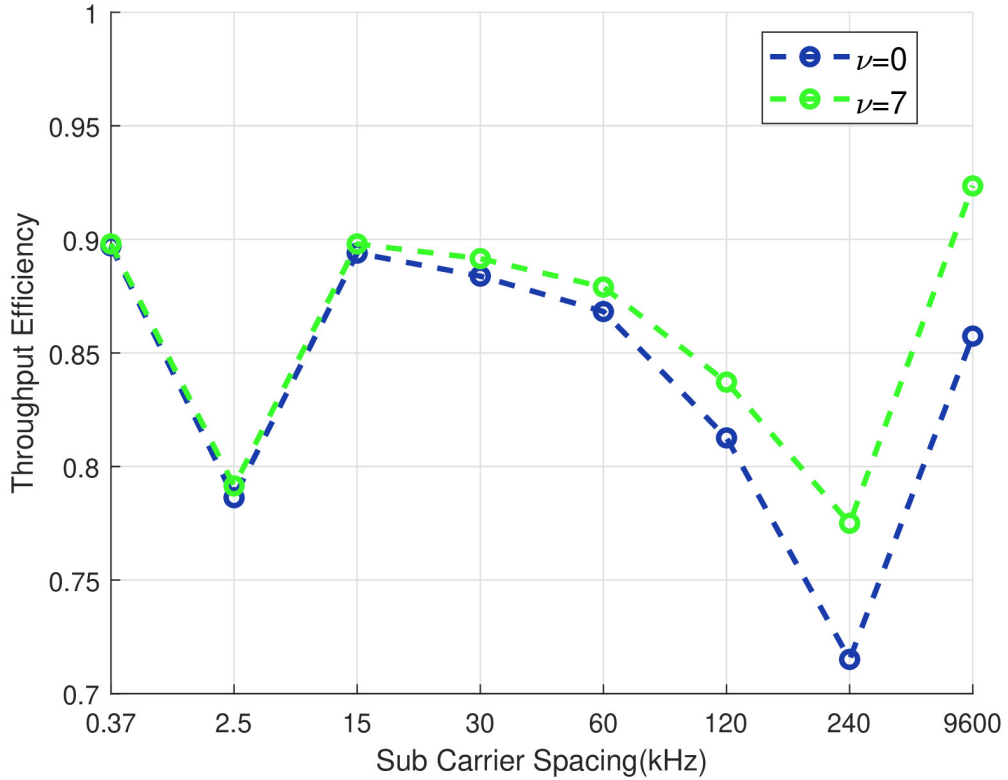


Figure 3.4: Throughput efficiency versus the sub-carrier spacing for 5G broadcasting, 5G NR numerologies and single carrier spacing with SNR=5dB; TDL-A DS=50 μ s (HPHT1, NLOS, 125km ISD)

3.3.3 Performances of realistic system

In this section, we present our results of the practical full link which comprises of a standard 5G NR LDPC encoder with code rate 0.53, a Mapper to 4QAM, 16QAM or 64QAM modulation, an OFDM modulator and the TDL-A channel. The considered target spectral efficiencies are then 1.06, 2.12, 3.18 bit/s/Hz, respectively.

The Bit Error Rate (BER) for the three considered receiver schemes is reported in Figure 3.6 with the same convention used in Figure 3.5. The realistic link results confirm the pragmatic capacity results in Figure 3.5. The performance of the 2D-MMSE equalizer with 15 kHz carrier spacing is similar to that of a single tap equalizer with 0.37 kHz carrier spacing and with a long CP length. On the other hand, a single tap equalizer with 15 kHz carrier spacing and short CP length (less than 5 μ s) can not compensate channel effect. Since the achievable information rate, in this case, is below one and target spectral efficiency equal to 1.06 bit/s/Hz,

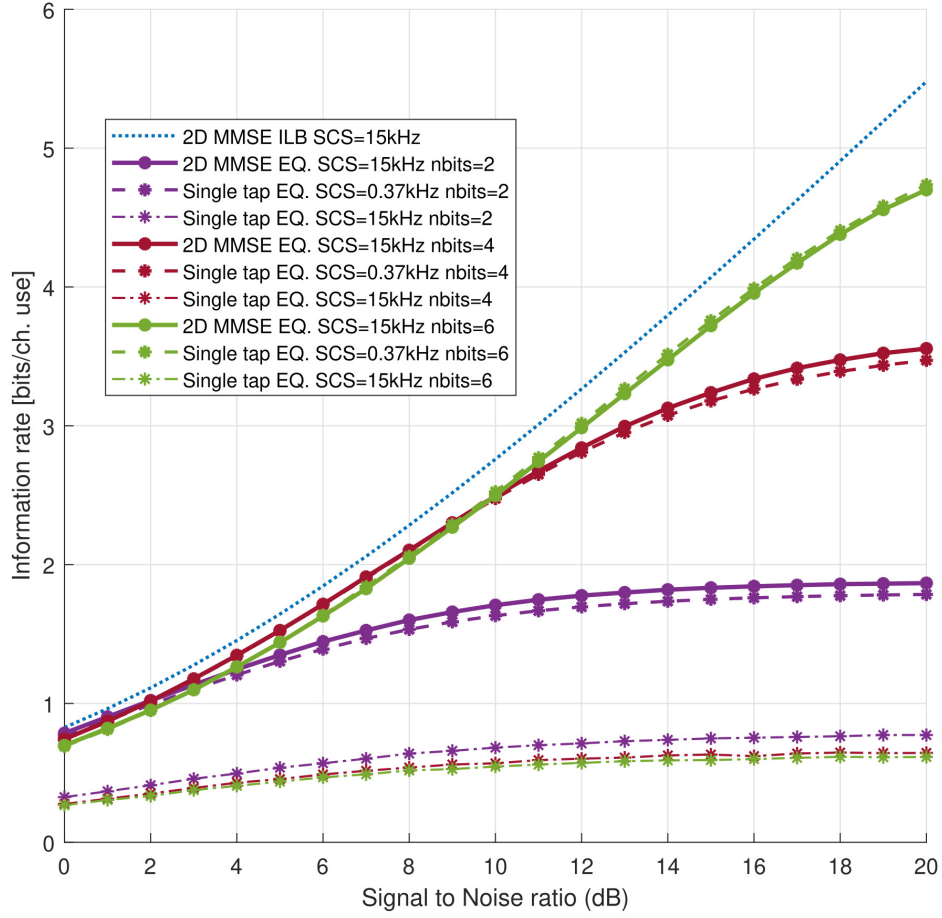


Figure 3.5: Pragmatic capacity of QPSK, 16QAM and 64QAM inputs for single tap and 2D-MMSE equalizer

increasing signal to noise ratio can not improve BER.

The SNR thresholds at 1% Block Error Rate (BLER) for LPLT, MPMT and HPHT SFNs networks are shown in Figure 3.7 for the 2D-MMSE and single tap receiver system with 15 and 0.37 kHz carrier spacing, respectively. In all SFN network scenarios, the 2D-MMSE equalizer outperforms the single tap equalizer with a long CP length ($300\mu s$). The 2D-MMSE performance is uniform in the considered delay spread range and doesn't degrade significantly by increasing the delay spread, so that it may be used also in more challenging scenarios HPHT2 with $75\mu s$ delay spread. The 2D-MMSE thus provides an attractive and simple single solution for all SFN networks using 5G NR numerologies.

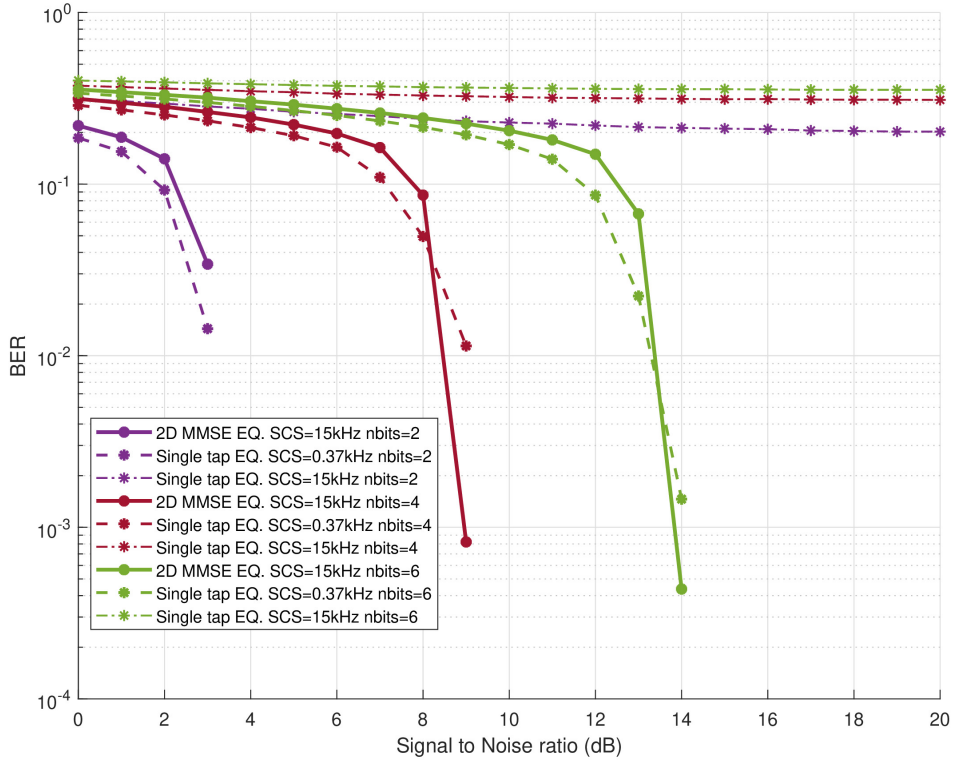


Figure 3.6: Simulated BER of the three considered realistic systems over TDL-A DS=50 μ s (HPHT1, NLOS, 125km ISD)

it is demonstrated the feasibility of using 5G NR numerologies in the deployment of efficient SFN networks for delivering TV broadcasting services.

In order to achieve this goal, We equalized the ISI/ICI channel using a properly designed 2D-MMSE filter (per tone time/frequency filter) instead of a typical single tap equalizer that can be used only with long CP overhead.

The design of the optimal 2D-MMSE filter has been obtained along the procedure outlined in [14], which is valid for any linear channel. The procedure is based on the channel shortening principle and allows to optimally design, assuming Gaussian inputs, a receiver where a suitable filter precedes a trellis processor with bounded state complexity. We provided a general procedure for building the ISI/ICI channel matrix correspondent to the equivalent channel that includes OFDM processing at both TX and RX and use it in the framework of [14] to derive the optimal receiver structure.

The theoretical result of the 2D-MMSE filter with Gaussian inputs showed that with 15 kHz carrier spacing the information rate gets close to maximum channel

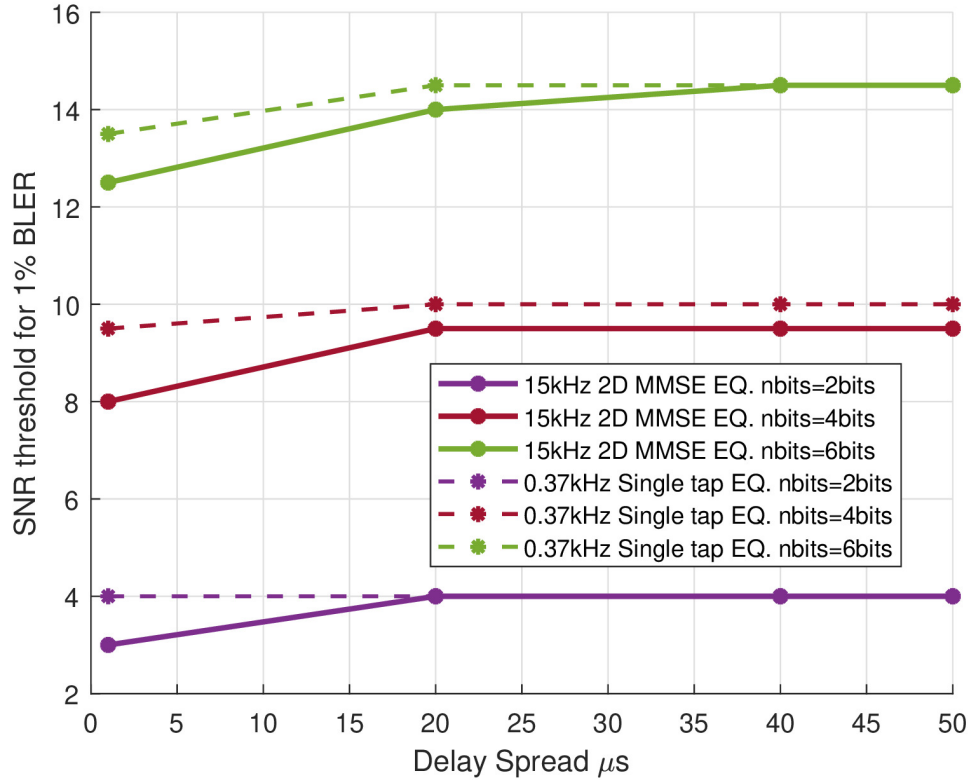


Figure 3.7: SNR thresholds (dB) at 1% BLER versus Delay spread of TDL-A channel model. Single Tap EQ. vs 2D-MMSE EQ. Code rate 0.53.

capacity even with the simplest low complexity receiver that does not require the adoption of an outer trellis processor. The low complexity 2D-MMSE with 15 kHz carrier spacing provided higher throughput efficiency versus single carrier and the other 5GNR numerologies. The pragmatic capacity associated with practical modulation confirmed the theoretical results.

For the considered SFN network scenarios, single tap equalization with 5GNR numerologies provides very poor performances due to the unacceptable ISI/ICI conditions. On the other hand, the adoption of 2D-MMSE filter allows to completely recover the performance losses and provides performances even better than those that can be obtained with OFDM parameters specifically designed for SFN networks [18], requiring much lower carrier spacing and longer CP length.

The presented results are promising but based on the very strong assumption of perfect channel knowledge at the receiver. In practice is well known that channel estimation is a very crucial function for the receiver performances, especially in a mobile environment.

Notice that the adoption of the shorter OFDM symbol associated with 5G NR numerologies is also expected to be more suitable in a mobile scenario, where the coherence time of the channel may become too short with respect to the OFDM symbol length.

in the following, it is explained more detail about equalization and adaptive methods. Then, the design of low complexity and adaptive 2-D channel equalizer will be considered which can acquire and track the ISI/ICI channel also in highly mobile environments. The crucial parameter that will be considered for complexity will be the number and positions of the required active taps in both dimensions and their trade-off with performance.

3.4 Performance of the 2-D Adaptive MMSE Equalizer

In this section, the performance of a low complex 2-D MMSE equalizer and the effects of changing different parameters on performance are considered. The simulation is performed on the OFDM system with the "TDL" channel model and the mean square error is the criteria in which we can see the performances and differences in the behavior of equalizer based on changing the parameters such as delay spread, size, and form of the active taps.

The result is based on an OFDM system that works with 4-QAM modulation and a "TDL" channel model. Here we consider "TDL-A channel profile with NLOS. In this system, we are using the 40 sub-carrier with a bandwidth equal to 15 kHz. The Delay spread is equal to 10 μs and the channel has no speed.

As it is explained in chapter 2, the important criterion is the position of active taps in which we want to perform equalization. This can be selected by shapes such as a cross, circular, rectangular, or rhombic window, or even different shapes based on the norm vector space. Since there is a trade-off between complexity and performance, according to the norm space, it is possible to consider many shapes. Therefore we can choose the proper shape to acquire affordable performance compared with complexity. In the next section, first, we compared two different shapes with different sizes of the window but with the same complexity of computation. Then we compare the different windows with the same size and different complexity and we represent the effects of the learning rate of the equalizer. Finally, we illustrate the comparison between the performance of the adaptive algorithm and the optimal value that is obtained by optimal channel shortening in chapter 2.

A. Same complexity Performances

Considering the functionality of an equalizer with different shapes at the same complexity can give us the perspective to choose the best shape for equalization. This is important because, In the same complexity, it is possible to find which shape involves more relevant active taps. The simulation is done for two rectangular and cross shapes. For the rectangular shape, the window entails 8 sub-carrier with the memory of channel equal to 4, ($N \times L = 8 \times 4$) while, for the cross shape the window contains ($N \times L = 13 \times 20$). Therefore, both Sets of taps have the same number of elements. The Delay spread and SNR are $10 \mu s$ and 10 dB respectively and there is no speed. Figure 3.8 shows the Mean square error versus the number of iteration. As it is illustrated the rectangular shape contains more relevant active Taps and has better functionality with respect to the cross set of the taps. The algorithm is designed flexibly such that there is the possibility to choose the different shapes of the window to find the best choice by determining the order of the norm of the vector.

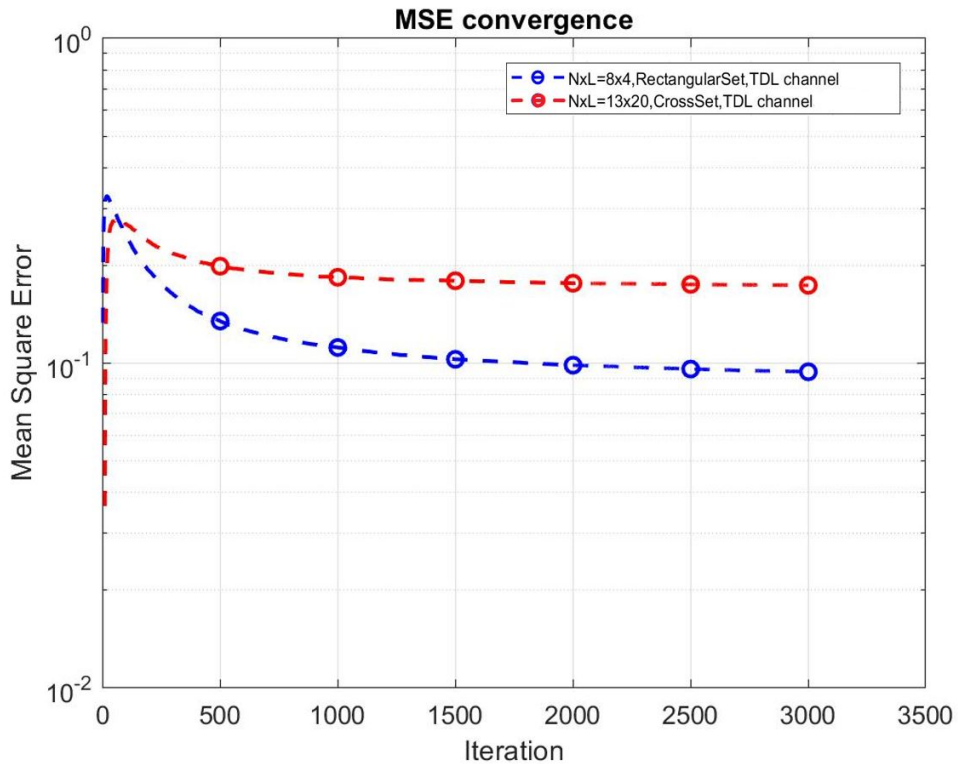


Figure 3.8: Mean Square Error versus the number of Iteration with same complexity for different shapes and different size of the window for OFDM system with "TDL-A channel model.

B. Comparison windows with Different complexity

In this part, the result is illustrated considering the same size of the window for different shapes of the active taps. It is important to find with the same size of the window, which shape propose the better performance. Figure 3.9 is shown the differences in choosing the rectangular and cross shape for a window of active taps with size ($N \times L = 8 \times 4$). The rectangular form of active taps consider more taps that are relevant and have the better result compared with cross shape, but it has a higher complexity of computation.

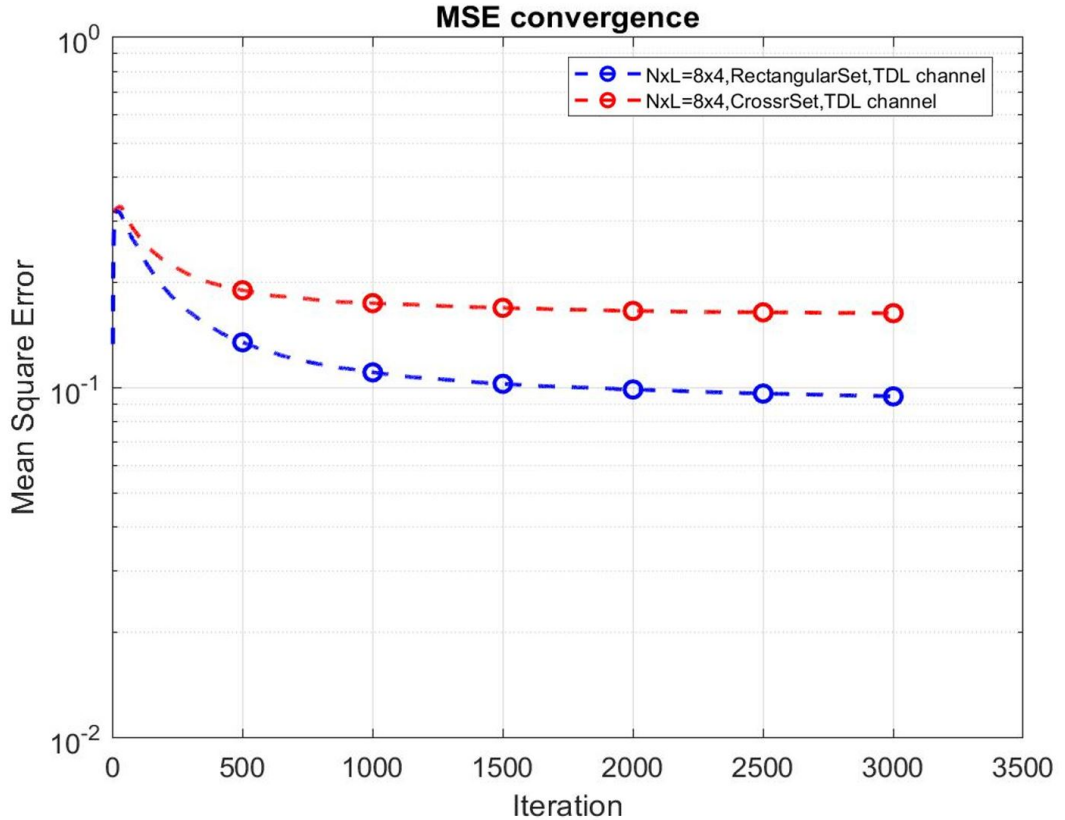


Figure 3.9: Mean Square Error versus the number of Iteration with the same size of window (8×4) and different shape for OFDM system with "TDL-A" channel model with SNR=10dB; DS = $10e-6$.

For the different complexity, it is also possible to illustrate the effect of having the greater window of active taps in the same shape. By increasing the size of the window and considering larger tap coefficients, it is expected to have a better result. Considering more related neighbors as active taps can make the better

performance. Especially in the system in which there is intersymbol interference, the effect of the window size would be more important. Figure 3.10 explained the difference in performance when we increase the $\mathbf{N} \times \mathbf{L}$ window from 2×2 to 8×4 . As it is expected, the effect of increasing the size of the window is more obvious for the rectangular shape than the cross shape. Because the number of tap coefficients is changed from 4 elements to 32 elements while in the cross shape the coefficients increase from 3 to 11. Therefore, the complexity of the rectangular shape is increased much more than the cross shape and despite the better result, choosing the large window in this shape can impose a huge complexity.

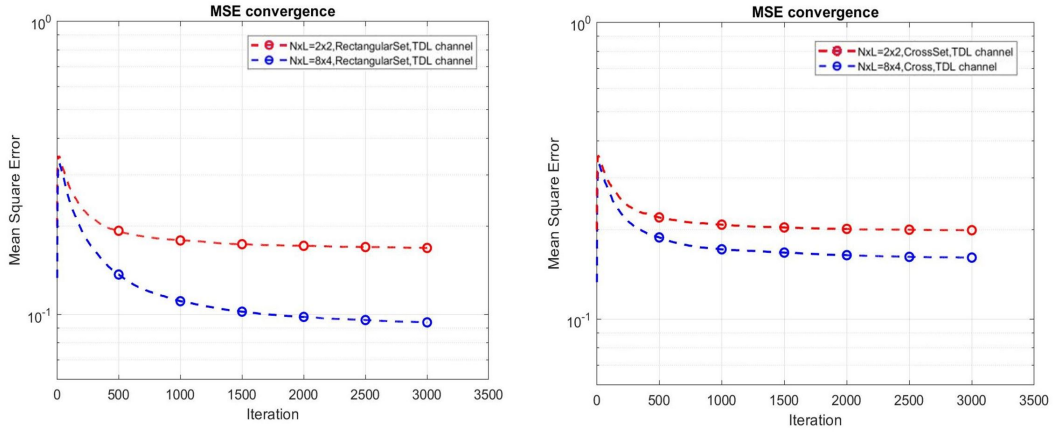


Figure 3.10: Mean Square Error versus the number of Iteration with different window size for Cross and Rectangular shape with OFDM system with "TDL-A" channel model with SNR=10dB; DS = $10e-6$; step size = 0.01.

It should be noticed, having a great window and many active taps in the equalization process is not always improve the performance. This criterion should be selected base on the system parameters and environment conditions. because the residual MSE can be grown by a number of taps as well as the step size ($\text{MSE} \propto \alpha^2 \mathbf{N}$). Therefore, there is a trade-off in choosing the number of taps which depends on the requirement of the system. As a result, Selecting the size of the window could be a parameter that leads to having an optimal equalizer by changing dynamically based on the condition.

C. Learning rate of the equalizer

The Learning rate of the equalizer defines how fast the algorithm of the equalizer converges to the optimal value. This rate is used to update the tap coefficients. Based on the value of the learning rate, we can find how fast the algorithm converges

to the desired value. Figure 3.11 shows the differences in the convergence between two different learning rates.

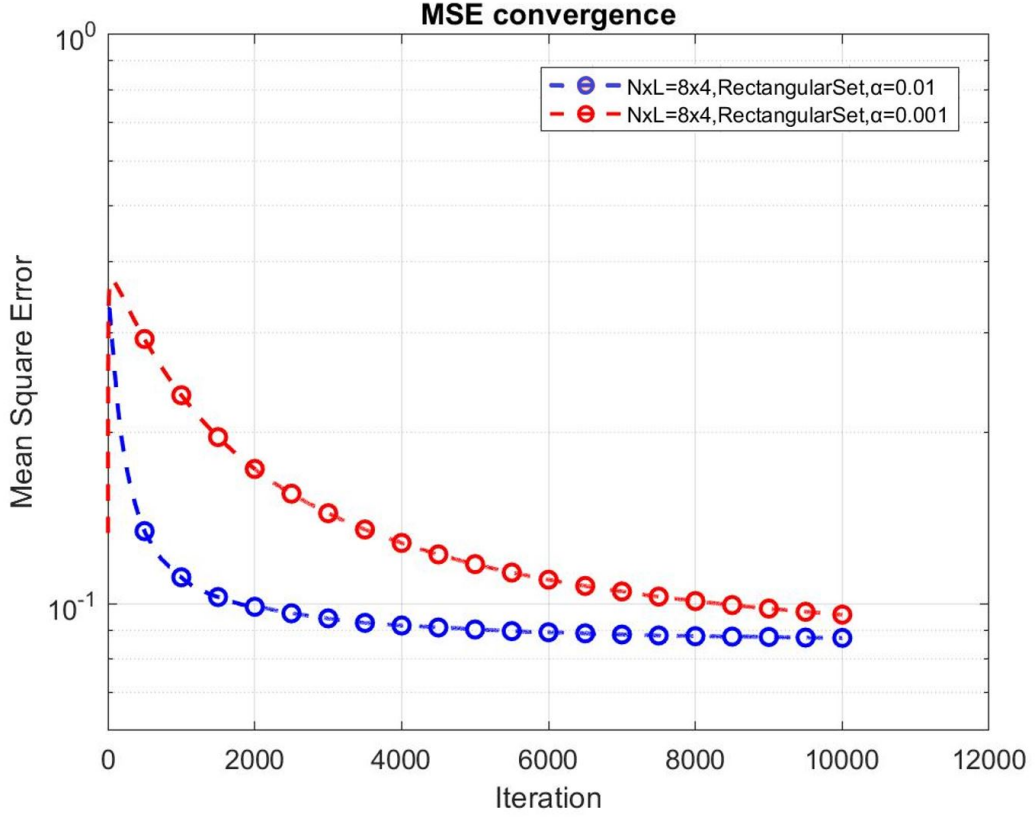


Figure 3.11: Mean Square error convergence for different learning rate.

It can be seen in Figure 3.11, by taking the larger value of learning rate, the solution is converged faster such that the MSE is below 0.15 for learning rate 0.01 after 500 iterations while this value is obtained after about 2900 iterations for a learning rate equal to 0.001. Selecting the large value of the learning rate could bring faster convergence but the possibility of diverging will be increased. While smaller step size could guarantee convergence with lower speed. Figure 3.12 is illustrated how fast the Convergence of the adaptive algorithm happens. In this figure, we increase the learning rate from 0.001 to 0.021. With blue curve, we can see on which iteration the algorithm converges and it is obvious, The convergence is faster for a large value of learning rate. On the other hand, the red curve shows by increasing the learning rate, the residual mean square error is increasing. Therefore, there is a trade-off to choose the appropriate value for the learning rate.

There is a solution in which we can choose the learning rate dynamically, in such

a way at the beginning we can use a large rate in order to have a fast convergence and then, after some iteration the rate decreases to make a smaller mean square error.

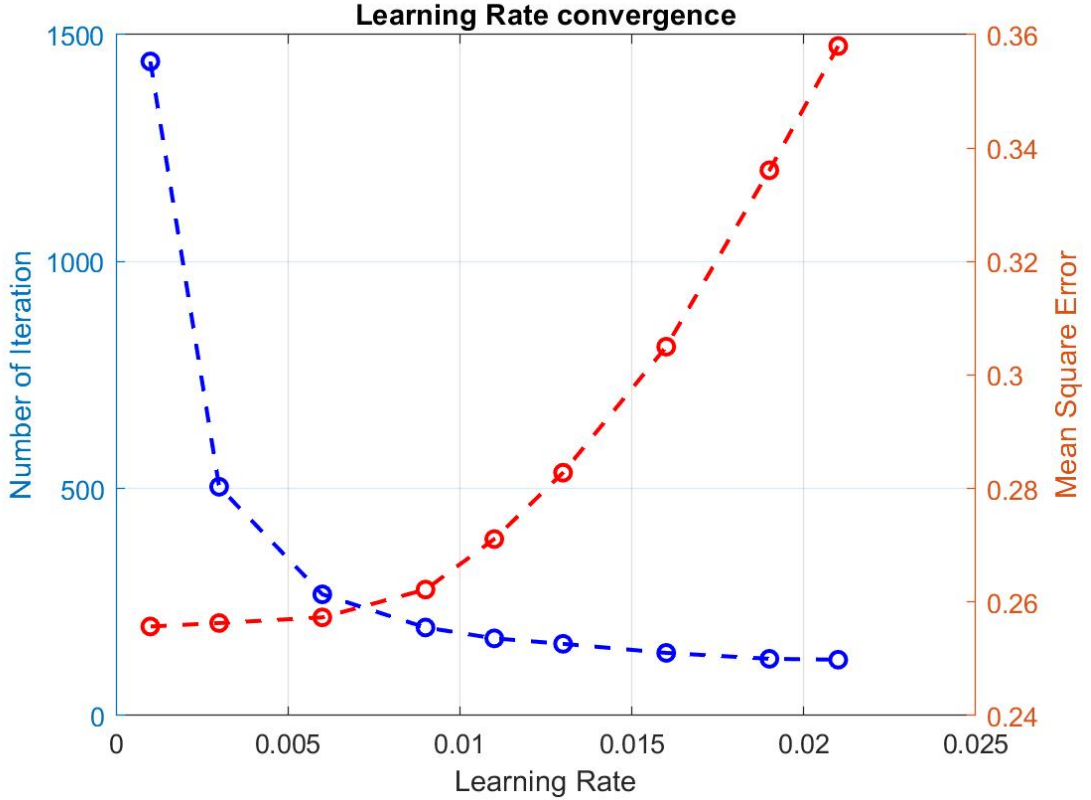


Figure 3.12: Speed of convergence versus increasing the learning rate of equalizer (blue curve) and Residual MSE versus increasing the learning rate of equalizer (red curve) with SNR = 7dB and DS =10 μ s.

D. Comparing with the Optimal filter

The design of the optimal 2D-MMSE filter has been obtained in section 2.2.1 along the procedure outlined in [14], in which the optimal receiver is characterized by an optimal $\tilde{\mathbf{H}}^r$ filter given by Equation 2.21 which is a standard MMSE/Wiener filter compensated by trellis processor represented by matrix $\tilde{\mathbf{G}}^r$. This is valid for any linear channel. Figure 3.13 compares the value of the Mean square Error obtained by the optimal MMSE/Wiener filter and the 2-D adaptive filter. AS it is obvious, the MSE of the adaptive algorithm is close to the optimal value and it might be closer if we change the parameters of the system such as shape and size of the

active taps, learning rate, etc.

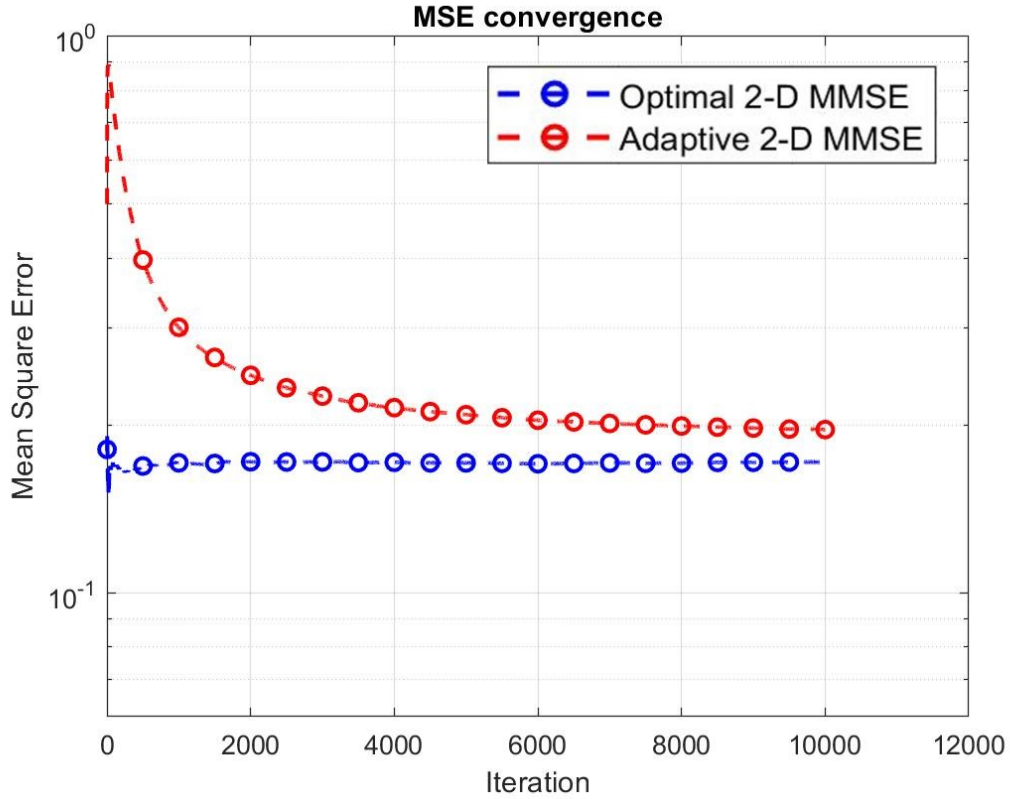


Figure 3.13: Comparison the Mean Square Error of the optimal EQ. versus Adaptive 2-D MMSE EQ. for SNR = 7dB and DS = 10 μ s.

3.5 Conclusion and Future Work

In this thesis, we demonstrated the feasibility of using 5G NR numerologies in the deployment of efficient SFN networks for delivering TV broadcasting services.

In order to achieve this goal, We equalized the ISI/ICI channel using a properly designed 2D-MMSE filter (per tone time/frequency filter) instead of a typical single tap equalizer that can be used only with long CP overhead.

The design of the optimal 2D-MMSE filter has been obtained along the procedure outlined in [14], which is valid for any linear channel. The procedure is based on the channel shortening principle and allows to optimally design, assuming Gaussian inputs, a receiver where a suitable filter precedes a trellis processor with bounded state complexity. We provided a general procedure for building the ISI/ICI channel

matrix correspondent to the equivalent channel that includes OFDM processing at both TX and RX and uses it in the framework of [14] to derive the optimal receiver structure.

The theoretical result of the 2D-MMSE filter with Gaussian inputs showed that with 15 kHz carrier spacing the information rate gets close to maximum channel capacity even with the simplest low complexity receiver that does not require the adoption of an outer trellis processor. The low complexity 2D-MMSE with 15 kHz carrier spacing provided higher throughput efficiency versus single carrier and the other 5G NR numerologies. The pragmatic capacity associated with practical modulation confirmed the theoretical results.

For the considered SFN network scenarios, single tap equalization with 5G NR numerologies provides very poor performances due to the unacceptable ISI/ICI conditions. On the other hand, the adoption of 2D-MMSE filter allows to completely recover the performance losses and provides performances even better than those that can be obtained with OFDM parameters specifically designed for SFN networks [18], requiring much lower carrier spacing and longer CP length.

Notice that the adoption of the shorter OFDM symbol associated to 5G NR numerologies is also expected to be more suitable in mobile scenario, where the coherence time of channel may become too short wrt the OFDM symbol length.

The presented results are promising but based on the very strong assumption of perfect channel knowledge at the receiver. In practice it is well known that channel estimation is a very crucial function for the receiver performances, especially in a mobile environment.

Then, we presented our results of implementing a low complexity 2-D adaptive MMSE equalizer in different systems with the OFDM system and the "TDL" channel model and demonstrated how it is possible to improve the performance by adjusting different parameters.

We presented the different possibilities for choosing the active taps in order to decrease the complexity by selecting more relevant taps. For this purpose, we introduced different shapes based on the norm of the vector space, and we compared rectangle and cross sets of taps to show the differences. First, we compared the two shapes in the same complexity, which means the size of the window is chosen in such a way the number of taps is equal for both shapes. Then, the comparison is illustrated based on different complexity with the same size of the window and we have seen in both cases the rectangular shape of the taps has better performance.

For the next step, we considered the effect of adjusting the learning rate on the convergence of the MSE. It is illustrated by increasing the learning rate, the convergence of the MSE is faster however the value of residual MSE is increased. Therefore, there is a trade-off in selecting the proper learning rate for the equalizer. Finally, we compared the performance of the 2-D adaptive equalizer with the optimal MMSE equalizer which is obtained in chapter 2 and we found that the

adaptive equalizer works close enough to the optimal value.

Our future work will then be devoted to demonstrate the performance of the equalizer in a practical full link and illustrate the performance by measuring the throughput. Based on the system implementation, it is possible to change the parameters of the equalizer to have the optimal solution and better performance considering the reasonable complexity of computation. Moreover, it is possible to implement and design the equalizer using Neural Networks and Deep Learning concepts which are expected to have a better result compared with linear equalization.

Bibliography

- [1] Ayan Sengupta, Alberto Rico Alvarino, Amer Catovic, and Lorenzo Casaccia. «Cellular terrestrial broadcast—Physical layer evolution from 3GPP release 9 to release 16». In: *IEEE Transactions on Broadcasting* 66.2 (2020), pp. 459–470 (cit. on pp. 2, 25, 26).
- [2] Agnes Ligeti. *Single Frequency Network planning*. 1999 (cit. on pp. 2, 3).
- [3] Madhu.A. «DSP Implementation OF OFDM Acoustic Modem». 2008 (cit. on pp. 3, 4).
- [4] Ke-Lin Du and M. N. S Swamy. *Wireless Communication Systems - From RF Subsystems to 4G Enabling Technologies*. Cambridge: Cambridge University Press, 2010. ISBN: 9780521114035 (cit. on pp. 11, 13–15).
- [5] H. C. Myburgh and J. C. Olivier. «Low Complexity MLSE Equalization in Highly Dispersive Rayleigh Fading Channels». In: *EURASIP Journal on Advances in Signal Processing* 2010 (2010) (cit. on p. 11).
- [6] Simon Haykin. *Adaptive filter theory, 5th edition*. Pearson Education, 2014. ISBN: 9780273764083 (cit. on p. 15).
- [7] B.Farhang-Boroujeny. *Adaptive Filters: Theory and Application*. John Wiley & Sons, 1998 (cit. on p. 15).
- [8] Malik Garima and Singh Sappal mandeep. «Adaptive Equalization Algorithms:An Overview». In: *International Journal of Advanced Computer Science and Applications* 2.3 (2011), pp. 62–67 (cit. on pp. 15–17).
- [9] Paulo S. R. Diniz. *Adaptive Filtering, Algorithms and Practical Implementation*. Springer Nature Switzerland, 2020. ISBN: 978-3-030-29057-3 (cit. on pp. 16, 18).
- [10] John E. Kleider and Xiaoli Ma. «Adaptive channel shortening equalization for coherent OFDM doubly selective channels». In: *IEEE* 06 (2006), pp. 361–364 (cit. on pp. 18, 19).
- [11] David D Falconer and FR Magee Jr. «Adaptive channel memory truncation for maximum likelihood sequence estimation». In: *Bell System Technical Journal* 52.9 (1973), pp. 1541–1562 (cit. on pp. 19, 26).

- [12] Jacky S. Chow, Jerry C. Tu, and John M. Cioffi. «A discrete multitone transceiver system for HDSL applications». In: *IEEE journal on selected areas in communications* 9.6 (1991), pp. 895–908 (cit. on pp. 19, 26).
- [13] Katleen Van Acker, Geert Leus, Marc Moonen, Olivier Van de Wiel, and Thierry Pollet. «Per tone equalization for DMT-based systems». In: *IEEE transactions on communications* 49.1 (2001), pp. 109–119 (cit. on pp. 19, 20).
- [14] Fredrik Rusek and Adnan Prlja. «Optimal channel shortening for MIMO and ISI channels». In: *IEEE transactions on wireless communications* 11.2 (2011), pp. 810–818 (cit. on pp. 19, 20, 24, 26, 29, 35, 42–44).
- [15] Wei Wu Habtamu Zegeye Alemu and Junhong Zhao. «Feedforward Neural Networks with a Hidden Layer Regularization Method». In: (2018) (cit. on p. 23).
- [16] D Vargas and D Mi. «LTE-Advanced pro broadcast radio access network benchmark». In: *Deliverable D3 1* (2017), pp. 197–203 (cit. on p. 25).
- [17] Inaki Eizmendi, Manuel Velez, David Gómez-Barquero, Javier Morgade, Vicente Baena-Lecuyer, Mariem Slimani, and Jan Zoellner. «DVB-T2: The second generation of terrestrial digital video broadcasting system». In: *IEEE transactions on broadcasting* 60.2 (2014), pp. 258–271 (cit. on p. 25).
- [18] “*Study on LTE-based 5G terrestrial broadcast (release 16)*” 3GPP, Sophia Antipolis, France, Rep. 3GPP TR 36.776 (cit. on pp. 26, 27, 36, 44).